Geographic variability in freshwater methane hydrogen isotope ratios and its implications for global isotopic source signatures

Peter M.J. Douglas[1], Emerald Stratigopoulos[1*], Jenny Park[1], Dawson Phan[1]

[1]Earth and Planetary Sciences, McGill University, Montreal, H3A 0E8, Canada
* Now at Department of Earth Sciences, University of Toronto, Toronto, M5S 3B1, Canada

Correspondence to: Peter M. J. Douglas (peter.douglas@mcgill.ca)

Abstract. There is growing interest in developing spatially resolved methane (CH_4) isotopic source signatures to aid in geographic source attribution of CH_4 emissions. CH_4 hydrogen isotope measurements (δ^2H-CH_4) have the potential to be a powerful tool for geographic differentiation of CH_4 emissions from freshwater environments, as well as other microbial sources. This is because microbial δ^2H-CH_4 values are partially dependent on the δ^2H of environmental water (δ^2H-H_2O), which exhibits large and well-characterized spatial variability globally. We have refined the existing global relationship between δ^2H-CH_4 and δ^2H-H_2O by compiling a more extensive global dataset of δ^2H-CH_4 from freshwater environments, including wetlands, inland waters, and rice paddies, comprising a total of 129 different sites, and compared these with measurements and estimates of δ^2H-H_2O, as well as $\delta^{13}C$-CH_4 and $\delta^{13}C$-CO_2 measurements. We found that estimates of δ^2H-H_2O explain approximately 42% of the observed variation in δ^2H-CH_4, with a flatter slope than observed in previous studies. The inferred global δ^2H-CH_4 vs. δ^2H-H_2O regression relationship is not sensitive to using either modelled precipitation δ^2H or measured δ^2H-H_2O as the predictor variable. The slope of the global freshwater relationship between δ^2H-CH_4 and δ^2H-H_2O is similar to observations from incubation experiments, but is different from pure culture experiments. This result is consistent with previous suggestions that variation in the δ^2H of acetate, controlled by environmental δ^2H-H_2O, is important in determining variation in δ^2H-CH_4. The relationship between δ^2H-CH_4 and δ^2H-H_2O leads to significant differences in the distribution of freshwater δ^2H-CH_4 between the northern high latitudes (60-90ºN), relative to other global regions. We estimate a flux-weighted global freshwater δ^2H-CH_4 of -310±15‰, which is higher than most previous estimates. Comparison with $\delta^{13}C$ measurements of both CH_4 and CO_2 implies that residual δ^2H-CH_4 variation is the result of complex interactions between CH_4 oxidation, variation in the dominant pathway of methanogenesis, and potentially other biogeochemical variables. We observe a significantly greater distribution of δ^2H-CH_4 values, corrected for δ^2H-H_2O, in inland waters relative to wetlands, and suggest this difference is caused by more prevalent CH_4 oxidation in inland waters. We used the expanded freshwater CH_4 isotopic dataset to calculate a bottom-up estimate of global source δ^2H-CH_4 and $\delta^{13}C$-CH_4 that includes spatially resolved isotopic signatures for freshwater CH_4 sources. Our bottom-up global source δ^2H-CH_4 estimate (-278±15‰) is higher than a previous estimate using a similar approach, as a result of the more enriched global freshwater δ^2H-CH_4 signature derived from our dataset. However, it is

32   in agreement with top-down estimates of global source δ^2H-CH$_4$ based on atmospheric measurements and estimated

33   atmospheric sink fractionations. In contrast our bottom-up global source δ^{13}C-CH$_4$ estimate is lower than top-down

34   estimates, partly as a result of a lack of δ^{13}C-CH$_4$ data from C$_4$ plant dominated ecosystems. In general, we find there is a

35   particular need for more data to constrain isotopic signatures for low-latitude microbial CH$_4$ sources.

1 Introduction

37   Methane (CH$_4$) is an important greenhouse gas that accounts for approximately 25% of current anthropogenic global

38   warming, but we do not have a complete understanding of the current relative or absolute fluxes of different CH$_4$ sources

39   to the atmosphere (Schwietzke et al., 2016;Saunois et al., 2019), nor is there consensus on the causes of recent decadal-

40   scale changes in the rate of increase in atmospheric CH$_4$ (Kai et al., 2011;Pison et al., 2013;Rice et al., 2016;Schaefer et

41   al., 2016;Worden et al., 2017;Thompson et al., 2018;Turner et al., 2019). Freshwater ecosystems are an integral

42   component of the global CH$_4$ budget. They are one of the largest sources of atmospheric CH$_4$ and are unequivocally the

43   largest natural, or non-anthropogenic, source (Bastviken et al., 2011;Saunois et al., 2019). At the same time the

44   geographic distribution of freshwater CH$_4$ emissions, changes in the strength of this source through time, and the relative

45   importance of wetland versus inland water CH$_4$ emissions all remain highly uncertain (Pison et al., 2013;Schaefer et al.,

46   2016;Ganesan et al., 2018;Saunois et al., 2019;Turner et al., 2019). Gaining a better understanding of freshwater CH$_4$

47   emissions on a global scale is of great importance for understanding potential future climate feedbacks related to CH$_4$

48   emissions from these ecosystems (Bastviken et al., 2011;Koven et al., 2011;Yvon-Durocher et al., 2014;Zhang et al.,

49   2017). It is also necessary in order to better constrain the quantity and rate of change of other CH$_4$ emissions sources,

50   including anthropogenic sources from fossil fuels, agriculture, and waste (Kai et al., 2011;Pison et al., 2013;Schaefer et

51   al., 2016).

52   Isotopic tracers, particularly δ^{13}C, have proven to be very useful in constraining global CH$_4$ sources and sinks

53   (Kai et al., 2011;Nisbet et al., 2016;Rice et al., 2016;Schaefer et al., 2016;Schwietzke et al., 2016;Nisbet et al., 2019).

54   However, δ^{13}C source signatures cannot fully differentiate CH$_4$ sources, leaving residual ambiguity in source

55   apportionment (Schaefer et al., 2016;Schwietzke et al., 2016;Worden et al., 2017;Turner et al., 2019). Applying

56   additional isotopic tracers to atmospheric CH$_4$ monitoring has the potential to greatly improve our understanding of CH$_4$

57   sources and sinks (Turner et al., 2019; Saunois et al., 2020). Recently developed laser-based methods, including cavity

58   ringdown spectroscopy, quantum cascade laser absorption spectroscopy, and tunable infrared laser direct absorption

59   spectroscopy, in addition to continued application of isotope ratio mass spectrometry (Chen et al., 2016; Röckmann et al.,

60   2016; Yacovitch et al., 2020) could greatly enhance the practicality of atmospheric δ^2H-CH$_4$ measurements at greater

61   spatial and temporal resolution, similar to recent developments for δ^{13}C-CH$_4$ measurements (Zazzeri et al., 2015; Miles et

62   al., 2018). δ^2H-CH$_4$ measurements have proven useful in understanding past CH$_4$ sources in ice-core records (Whiticar

and Schaefer, 2007; Mischler et al., 2009; Bock et al., 2010; Bock et al., 2017), but have seen only limited use in modern atmospheric CH_4 budgets (Kai et al., 2011; Rice et al., 2016), in part because of loosely constrained source terms, as well as relatively sparse atmospheric measurements. Atmospheric inversion models have shown that increased spatial and temporal resolution of δ^2H-CH_4 measurements could provide substantial improvements in precision for global and regional methane budgets (Rigby et al., 2012).

δ^2H-CH_4 measurements could prove especially useful in understanding freshwater CH_4 emissions. Freshwater δ^2H-CH_4 is thought to be highly dependent on δ^2H-H_2O (Waldron et al., 1999a; Whiticar, 1999; Chanton et al., 2006). Since δ^2H-H_2O exhibits large geographic variation as a function of temperature and fractional precipitation (Rozanski et al., 1993; Bowen and Revenaugh, 2003), δ^2H-CH_4 measurements have the potential to differentiate freshwater CH_4 sources by latitude. This approach has been applied in some ice core studies (Whiticar and Schaefer, 2007; Bock et al., 2010), but geographic source signals remain poorly constrained, in part because of small datasets and because of incompletely understood relationships between δ^2H-H_2O and δ^2H-CH_4. In contrast, recent studies of modern atmospheric δ^2H-CH_4 have typically not accounted for geographic variation in freshwater CH_4 sources (Kai et al., 2011; Rice et al., 2016). Relatedly, other studies have found an important role for variation in δ^2H-H_2O in controlling δ^2H-CH_4 from biomass burning (Umezawa et al., 2011) and from plants irradiated by UV light (Vigano et al., 2010), as well as the δ^2H of H_2 produced by wood combustion (Röckmann et al., 2016).

In addition to variance caused by δ^2H-H_2O, a number of additional biogeochemical variables have been proposed to influence δ^2H-CH_4 in freshwater environments. These include differences in the predominant biochemical pathway of methanogenesis (Whiticar et al., 1986; Whiticar, 1999; Chanton et al., 2006), the extent of methane oxidation (Happell et al., 1994; Waldron et al., 1999a; Whiticar, 1999; Cadieux et al., 2016), isotopic fractionation resulting from diffusive gas transport (Waldron et al., 1999a; Chanton, 2005), and differences in the thermodynamic favorability or enzymatic reversibility of methanogenesis (Valentine et al., 2004b; Stolper et al., 2015; Douglas et al., 2016). These influences on δ^2H-CH_4 have the potential to complicate geographic signals, but also provide the potential to differentiate ecosystem sources, if specific ecosystems are characterized by differing rates and pathways of methanogenesis, rates of CH_4 oxidation, or gas transport processes. A recent study proposed that freshwater $\delta^{13}C$-CH_4 could be differentiated geographically based on ecosystem differences in the prevalence of different methanogenic pathways and in the predominance of C_4 plants, in addition to the geographic distribution of wetland ecosystems (Ganesan et al., 2018). δ^2H-CH_4 measurements have the potential to complement this approach by providing an additional isotopic parameter for differentiating ecosystem and geographic CH_4 source signatures.

In order to use δ^2H-CH_4 as an indicator of freshwater ecosystem contributions to global and regional CH_4 emissions budgets, a clearer understanding of freshwater δ^2H source signals, and how they vary by geographic location, ecosystem type, and other variables is needed. In order to address this need we have assembled and analyzed a dataset of 897 δ^2H-CH_4 measurements from 129 individual ecosystems, or sites, derived from 40 publications (Schoell, 1983;

Woltemate et al., 1984; Burke Jr and Sackett, 1986; Whiticar et al., 1986; Burke Jr et al., 1988; Burke Jr, 1992; Burke Jr et al., 1992 ;Lansdown et al., 1992; Lansdown, 1992; Martens et al., 1992; Wassmann et al., 1992; Happell et al., 1993; Levin et al., 1993; Happell et al., 1994; Wahlen, 1994; Bergamaschi, 1997; Chanton et al., 1997; Hornibrook et al., 1997; Tyler et al., 1997; Zimov et al., 1997; Bellisario et al., 1999; Popp et al., 1999; Waldron et al., 1999b; Chasar et al., 2000; Marik et al., 2002; Nakagawa et al., 2002b; Nakagawa et al., 2002a; Chanton et al., 2006; Walter et al., 2006; Walter et al., 2008; Alstad and Whiticar, 2011; Brosius et al., 2012; Sakagami et al., 2012; Bouchard et al., 2015; Stolper et al., 2015; Wang et al., 2015; Cadieux et al., 2016; Douglas et al., 2016; Thompson et al., 2016; Lecher et al., 2017). We have advanced existing datasets of freshwater δ^2H-CH$_4$ (Whiticar et al., 1986; Waldron et al., 1999a; Sherwood et al., 2017) in the following key attributes: 1) compiling a significantly larger dataset than was previously available; 2) compiling paired δ^{13}C-CH$_4$ data for all sites, δ^{13}C-CO$_2$ data for 50% of sites, and δ^2H-H$_2$O data for 47% of sites; 3) compiling geographic coordinates for all sites, providing the ability to perform spatial analyses and compare with gridded datasets of precipitation isotopic composition; and 4) classifying all sites by ecosystem and sample type (dissolved vs. gas samples), allowing for a clearer differentiation of how these variables influence δ^2H-CH$_4$.

Using this data set we applied statistical analyses to address key questions surrounding the global distribution of freshwater δ^2H-CH$_4$, the variables that control this distribution, and its implications for atmospheric δ^2H-CH$_4$. Specifically, we investigated the nature of the global dependence of δ^2H-CH$_4$ on δ^2H-H$_2$O, and whether this relationship results in significant differences in freshwater δ^2H-CH$_4$ by latitude. We also assessed whether variability in δ^{13}C-CH$_4$, δ^{13}C-CO$_2$, and α_C was correlated with δ^2H-CH$_4$, and whether there are significant differences in δ^2H-CH$_4$ between different ecosystem and sample types. Finally, we used our dataset, combined with other isotopic datasets (Sherwood et al., 2017) and flux estimates (Saunois et al., 2020), to estimate the global δ^2H-CH$_4$ and δ^{13}C-CH$_4$ of global emissions sources, and compared this with previous estimates based on atmospheric measurements or isotopic datasets (Whiticar and Schaefer, 2007;Rice et al., 2016;Sherwood et al., 2017),.

2 Methods

2.1 Isotope Nomenclature

Hydrogen and carbon isotope ratios are primarily discussed as delta values, using the generalized formula (Coplen, 2011):

$$\delta = \frac{\left(R_{sample} - R_{standard}\right)}{R_{standard}} \tag{1}$$

where R is the ratio of the heavy isotope to the light isotope, and the standard is Vienna Standard Mean Ocean Water (VSMOW) for δ^2H and Vienna Pee Dee Belemnite (VPDB) for δ^{13}C. δ values are expressed in per mil (‰) notation.

125   We also refer to the isotopic fractionation factor between two phases, or α, which is defined as:

126    $$\alpha_{a-b} = \frac{R_a}{R_b} = \frac{\delta_a + 1}{\delta_b + 1}$$ (2)

127   Specifically, we discuss the carbon isotope fractionation factor between CO_2 and CH_4 (α_C) and the hydrogen isotope

128   fractionation factor between H_2O and CH_4 (α_H).

129   **2.2 Dataset Compilation**

130   **2.2.1 Literature Survey**

131   To identify datasets we used a set of search terms (methane OR CH_4 AND freshwater OR wetland OR peatland OR

132   swamp OR marsh OR lake OR pond OR 'inland water' AND 'hydrogen isotope' OR 'δD' OR 'δ^{2}H') in Google Scholar

133   to find published papers that discussed this measurement. We also identified original publications using previously

134   compiled datasets (Waldron et al., 1999a;Sherwood et al., 2017). Data for 90% of sites were from peer-reviewed

135   publications. Data from 13 sites were from a Ph.D. dissertation (Lansdown, 1992).

136   **2.2.2 Dataset structure**

137   Most samples were associated with geographic coordinates in data tables or text documentation, or with specific

138   geographic locations such as the name of a town or city. In a few cases we identified approximate geographic locations

139   based on text descriptions of sampling sites, with the aid of Google Earth software. Sampling sites were defined as

140   individual water bodies or wetlands as identified in the relevant study. In one study where a number of small ponds were

141   sampled from the same location, we grouped ponds of a given type as a single site (Bouchard et al., 2015). We divided

142   sampling sites into six ecosystem categories: 1) lakes and ponds (hereafter lakes), 2) rivers and floodplains (hereafter

143   rivers), 3) bogs, 4) fens, 5) swamps and marshes, and 6) rice paddies. Most data (7 of 8 sites) in the rivers category are

144   from floodplain lake or delta environments. Swamps and marshes were combined as one category because of a small

145   number of sites, and because there is no clear indication of biogeochemical differences between these ecosystems. To

146   make these categorizations we relied on site descriptions in the data source publications. We also analyzed data in two

147   larger environment types, inland waters (lakes and rivers) and wetlands (bogs, fens, swamps and marshes, and rice

148   paddies), which correspond to two flux categories (freshwaters and natural wetlands) documented by Saunois et al.

149   (2020). While rice paddies are an anthropogenic ecosystem, they are wetlands where microbial methanogenesis occurs

150   under generally similar conditions to natural wetlands, and therefore we included them as wetlands in our analysis. In

151   some cases the type of wetland was not specified. We did not differentiate between ombrotrophic and minerotrophic

152   peatlands since most publications did not specify this difference, although it has been inferred to be important for δ^{13}C-

CH$_4$ distributions (Hornibrook, 2009). For studies of bogs and fens that sampled by soil depth we have only included sample measurements from the upper 50 cm. This is based on the observation of large-scale isotopic variability with soil depth in these ecosystems (Hornibrook et al., 1997;Waldron et al., 1999b), and the observation that shallow peat is typically the dominant source of atmospheric emissions (Waldron et al., 1999b;Bowes and Hornibrook, 2006;Shoemaker et al., 2012), which is our primary focus in this study. Other wetland ecosystems were not sampled by soil depth.

We also categorized samples by the form in which CH$_4$ was sampled, differentiating between dissolved CH$_4$ and CH$_4$ emitted through diffusive fluxes, which we group as dissolved CH$_4$, and gas-phase samples, including bubbles sampled either by disturbing sediments or by collecting natural ebullition fluxes. In some cases the sampling method or type of sample was not specified, or samples were a mix of both categories, which we did not attempt to differentiate.

Where possible (78% of sites), δ^{2}H-CH$_4$ and δ^{13}C-CH$_4$ values, as well as δ^{13}C-CO$_2$ and δ^{2}H-H$_2$O, were gathered from data files or published tables. In a number of publications, representing 22% of sites, data were only available graphically. For these studies we used Webplot Digitizer (https://automeris.io/WebPlotDigitizer/) software to extract data for these parameters. Previous studies have shown that user errors from Webplot Digitizer are typically small, with 90% of user generated data within 1% of the actual value (Drevon et al., 2017). Based on this, we estimate a typical error for δ^{2}H-CH$_4$ data of less than 3‰. Studies where data were derived from graphs are identified in Supplementary Table S1 (Douglas et al., 2020).

2.2.3 Estimates of δ^{2}H-H$_2$O and its effects on δ^{2}H-CH$_4$

To estimate δ^{2}H-H$_2$O for sites where it was not measured we relied on estimates of the isotopic composition of precipitation (δ^{2}H$_p$), derived from the Online Isotopes in Precipitation Calculator v.3.1 (OIPC3.1; www.waterisotopes.org; Bowen and Wilkinson, 2002; Bowen and Revenaugh, 2003; Bowen et al., 2005). Inputs for δ^{2}H$_p$ estimates are latitude, longitude, and elevation. We estimated elevation for each site surface elevation at the site's geographic coordinates reported by Google Earth. We tabulated estimates of both annual and growing season precipitation-amount weighted δ^{2}H$_p$, where the growing season is defined as months with a mean temperature greater than 0 ºC. We then analysed whether annual or growing season δ^{2}H$_p$ is a better estimate of environmental δ^{2}H-H$_2$O for both wetlands and inland waters by comparing these values with measured δ^{2}H-H$_2$O for sites with measurements (See Sect. 3.2). Based on this analysis, we then identified a 'best-estimate' δ^{2}H-H$_2$O value for each site, using an approach similar to that of Waldron et al. (1999a). Namely, we apply measured δ^{2}H-H$_2$O where available, and estimates based on the regression analyses detailed in Section 3.2 for sites without measurements.

To account for the effects of δ^{2}H-H$_2$O on δ^{2}H-CH$_4$, we introduce the term δ^{2}H-CH$_{4,W0}$, which is the estimated δ^{2}H-CH$_4$ of a sample if it had formed in an environment where δ^{2}H-H$_2$O = 0‰. This is defined by the equation:

$$\delta^2\text{H-CH}_{4,\text{W0}} = \delta^2\text{H-CH}_4 - \left(b \times \delta^2\text{H}_2\text{O}\right) \tag{3}$$

184   where δ^2H-H$_2$O is the 'best-estimate' value for each site described above, *b* is the slope of the regression relationship of

185   δ^2H-H$_2$O vs. δ^2H-CH$_4$ for the entire dataset, as reported in Sect. 3.3. We also performed the same calculation separately

186   for the subset of sites with measured δ^2H-H$_2$O. We analyze δ^2H-CH$_{4,W0}$ instead of α_H because, as discussed in Sect. 3.3.1,

187   the global relationship between δ^2H$_p$ vs. δ^2H-CH$_4$ does not correspond to a constant value of α_H, and therefore deviations

188   from the global empirical relationship are more clearly expressed as a residual as opposed to a fractionation factor.

189

2.3 Statistical analyses

191   For all statistical analyses we use site-level mean isotopic values. This avoids biasing our analyses towards sites with a

192   large number of measurements, since there are large differences in the number of samples analyzed per site (*n* ranges

193   from 66 to 1). To calculate α_C we used average δ^{13}C-CH$_4$ and δ^{13}C-CO$_2$ at a given site. This approach entails some

194   additional uncertainty in this variable, but was necessary because at many sites these measurements were not made on the

195   same samples.

196   We perform a set of linear regression analyses δ^2H-CH$_4$ against other isotopic variables, in addition to latitude.

197   All statistical analyses were performed in Matlab. We considered $p < 0.05$ to be the threshold for identifying significant

198   regression relationships. We chose to perform unweighted regression, as opposed to weighted regression based on the

199   standard error of sample measurements, for two reasons. First, a small number of sites with a large number of

200   measurements, and therefore small standard error, had a disproportionate effect on weighted regression results. Second,

201   in environmental research unweighted regression is frequently less biased than weighted regression (Fletcher and Dixon,

202   2012). Based on a test proposed by Fletcher and Dixon (2012), unweighted regression is appropriate for this dataset. We

203   used analysis of covariance to test for significant differences between regression relationships.

204   To compare isotopic data (δ^2H-CH$_4$ and δ^{13}C-CH$_4$) between groups (i.e. latitudinal bands, ecosystem types,

205   sample types) we used non-parametric statistical tests to test whether the groups were from different distributions. We

206   used non-parametric tests because some sample groups were not normally distributed, as determined by a Shapiro-Wilk

207   test (Shapiro and Wilk, 1965). For comparing differences between the distributions of two groups we used the Mann-

208   Whitney U-test (Mann and Whitney, 1947), whereas when comparing differences between the distributions of more than

209   two groups we used the Kruskal-Wallis H-test (Kruskal and Wallis, 1952), combined with Dunn's test to compare

210   specific sample group pairs (Dunn, 1964). We considered $p < 0.05$ to be the threshold for identifying groups with

211   significantly different distributions.

212   When comparing δ^{13}C-CH$_4$ by latitude and ecosystem we combined the data from this study with additional data

213   from Sherwood et al. (2017) (32 additional sites) where δ^2H-CH$_4$ was not measured to make our dataset as representative

214   as possible. To our knowledge this combined dataset is the largest available compiled dataset of freshwater δ^{13}C-CH$_4$,

215   although there are many more δ^{13}C-CH$_4$ measurements that have not yet been aggregated. We did not include these

216 additional data when analysing differences by sample type, as sample type was not specified in the dataset of Sherwood
217 et al. (2017).

218 **2.4 Estimation of global atmospheric CH$_4$ δ^2H and δ^{13}C source values**

219 To better understand how latitudinal differences in wetland isotopic source signatures influence atmospheric δ^2H-CH$_4$
220 and δ^{13}C-CH$_4$, we calculated a 'bottom-up' mixing model of δ^2H-CH$_4$ and δ^{13}C-CH$_4$. For this calculation we ascribed all
221 CH$_4$ sources a flux (derived from Saunois et al., 2020; see details below) and a δ^2H and δ^{13}C value, and calculated the
222 global atmospheric source value using an isotopic mixing model. Because of non-linearity when calculating mixtures
223 using δ^2H values, we performed the mixing equation using isotopic ratios (see Sect. 2.1). The mixing equation is as
224 follows:

225 $$R_{mix} = f_1 R_1 + f_2 R_2 + ... + f_n R_n \qquad\qquad (4)$$

226 where f_n is the fractional flux for each source term (i.e. the ratio of the source flux to total flux), and R$_n$ is the isotope
227 ratio for each source term.

228 Values for the flux, δ^2H, and δ^{13}C applied for each source term are shown in Table 1. We used bottom-up source
229 fluxes from Saunois et al. (2020) for the period 2008-2017. For categories other than wetlands, inland waters, and rice
230 paddies, we used global fluxes and isotope values, since geographically resolved isotopic source signature estimates are
231 not available. For these sources we used δ^2H and δ^{13}C values published by Sherwood et al. (2017), using the mean value
232 for each source term. For wetlands, inland waters, and rice paddies, we used geographically resolved (60-90 ºN; 30-60
233 ºN, 90º S-30ºN) fluxes derived from Saunois et al. (2019) for the period 2008-2017, and mean δ^2H-CH$_4$ for these
234 latitudinal bands from this study.

235 To calculate mean δ^{13}C-CH$_4$ from wetlands, inland waters, and rice paddies for different latitudinal bands we
236 combined the data from this study along with additional data from Sherwood et al. (2017) (32 additional sites) to make
237 our estimated source signatures as representative as possible. To our knowledge this combined dataset is the largest
238 available compiled dataset of freshwater δ^{13}C-CH$_4$ (See Sect. 2.3). Sites dominated by C$_4$ plants are notably
239 underrepresented in this combined dataset. In addition, the biomass burning dataset of Sherwood e al. (2017) contains
240 very few data from C$_4$ plant combustion. We performed a separate estimate of global source δ^{13}C-CH$_4$ that attempted to
241 correct for these likely biases by making two adjustments: 1) using the estimated low-latitude wetland δ^{13}C-CH$_4$
242 signature of Ganesan et al., (2018) (-56.7‰), which takes into account the predicted spatial distribution of C$_4$ plant
243 dominated wetlands; and 2) using the biomass burning δ^{13}C-CH$_4$ signature of Schwietzke et al., (2016) (-22.3‰), which
244 is weighted by the predicted contribution from C$_4$ plant combustion. We did not attempt to take into account δ^{13}C-CH$_4$
245 from ruminants feeding on C$_4$ plants. For the C$_4$-plant corrected δ^{13}C-CH$_4$ estimate we applied the same uncertainties that
246 are reported in Table 1.

8

Table 1: Estimates of source-specific fluxes, δ²H-CH4, and δ¹³C-CH4, and their uncertainties, used in mixing models and Monte Carlo analyses

Category	Flux (Tg/Yr)	Uncertainty	δ^2H signature (‰, VSMOW)	Uncertainty	$\delta^{13}C$ signature (‰, VPDB)	Uncertainty
Wetlands (<30N)	115	37.5	-301	15	-64.4	1.9
Wetlands (30-60N)	25	16.5	-324	14	-61.8	2.6
Wetlands (>60N)	9	8.0	-374	10	-62.7	3.0
Inland Waters (<30N)	80	39.4	-301	12	-57.1	3.0
Inland Waters (30-60N)	64	31.9	-308	18	-62.0	3.8
Inland Waters (>60N)	16	7.5	-347	9	-65.0	1.8
Geological (onshore)[a]	38	13.0	-189	44	-43.8	10.0
Wild animals[b]	2	2.0	-316	28	-65.4	3.5
Termites[c]	9	6.0	-343	50	-63.4	3.5
Permafrost soils (direct)[d]	1	0.5	-374	15	-64.4	1.7
Geological (offshore)[a]	7	7.0	-189	44	-43.8	10.0
Biogenic open and coastal[e]	6	3.0	-200	50	-80.0	20.0
Enteric fermentation and manure	111	5.0	-308	28	-65.4	3.5
Landfills and waste	65	4.5	-297	6	-56.0	4.9
Rice cultivation (<30N)	19	1.2	-324	8	-55.0	6.5
Rice cultivation (30-60N)	12	0.5	-325	8	-62.3	2.1
Coal mining	42	15.5	-232	5	-49.5	1.0
Oil and gas	79	13.0	-189	2	-43.8	0.5
Industry[f]	3	3.0	-189	2	-43.8	0.5
Transport[f]	4	4.0	-189	2	-43.8	0.5
Biomass burning[g]	17	6.0	-211	15	-26.2	2.0
Biofuel burning[g]	12	2.0	-211	15	-26.2	2.0

a-No specific isotopic measurements in the database (Sherwood et al., 2017). We applied the mean isotopic values for oil and gas, and applied the standard deviation of for oil and gas as the uncertainty

b-No specific isotopic measurements in database (Sherwood et al., 2017). We used the isotopic values and uncertainties from livestock

c- Only one δ^2H measurement in database (Sherwood et al., 2017). We applied 50‰ as a conservative uncertainty estimate.

d- No specific isotopic measurement in database (Sherwood et al., 2017). We used the isotopic values and uncertainties for high-latitude wetlands

e- No specific isotopic measurements in database (Sherwood et al., 2017). We applied approximate isotopic values based on Whiticar, (1999), and conservatively large uncertainty estimates.

f-No specific isotopic measurements in database (Sherwood et al., 2017). We used the isotopic values and uncertainties for oil and gas.

g-We applied all isotopic measurements of biomass burning to both the biomass burning and biofuel burning categories. We did not correct for the relative proportion of C_3 and C_4 plant combustion sources (See Sect. 2.4)

247

248   Since fluxes from *other natural sources* are not differentiated for the period 2008-2017, we calculated the

249   proportional contribution of each category of other natural sources for the period 2000-2009 (Saunois et al., 2020), and

250   applied this to the total flux from other natural sources for 2008-2017. Inland waters and rice paddies do not have

251   geographically resolved fluxes reported in Saunois et al. (2020). Therefore, we calculated the proportion of *other natural*

252   *sources* attributed to inland waters from 2000-2009 (71%), and applied this proportion to the geographically resolved

253   fluxes of *other natural sources*. Similarly, we calculated the proportion of *agricultural and waste sources* attributed to

254   rice agriculture from 2008-2017 (15%), and applied this to the geographically resolved fluxes of *agricultural and waste*

255   *fluxes*.

256   To estimate uncertainty in the modelled total source δ^2H and δ^{13}C values we conducted Monte Carlo analyses

257   (Thompson et al., 1992). We first estimated the uncertainty for each flux, δ^2H, and δ^{13}C term. Flux uncertainties were

258   defined as one half of the range of estimates provided by Saunois et al., (2020). For sources where fluxes were calculated

259   as a proportion of a larger flux, we applied the same proportional calculation to uncertainty estimates. In cases where one

260   half of the range of reported studies was larger than the flux estimate, we set the uncertainty to be equal to the flux

261   estimate to avoid negative fluxes in the mixing model. Isotopic source signal uncertainties were defined as the 95%

262   confidence interval of the mean value for a given source category. For some sources there is insufficient data to calculate

263   a 95% confidence interval, and we applied a conservative estimate of uncertainty for these sources, as detailed in Table 1.

264   Confidence intervals for fossil fuel isotopic source signatures do not take into account variation in emissions fluxes and

265   isotopic values between regions or resource types (i.e. conventional vs. unconventional reservoirs). This variation is

266   difficult to quantify with available datasets, but could imply additional uncertainty in global source signatures. We

267   recalculated the δ^2H and δ^{13}C mixing models 10,000 times, each time sampling inputs from the uncertainty distribution

268   for each variable. We assumed all uncertainties were normally distributed. We interpret the 2-sigma standard deviation of

269   the resulting Monte Carlo distributions as an estimate of the uncertainty of our total atmospheric CH_4 source isotopic

270   values. To examine how the Monte Carlo analyses were specifically influenced by uncertainty in isotopic source

271   signatures vs. flux estimates, we conducted sensitivity tests where we set the uncertainty in either isotopic source

272   signatures or flux estimates to zero. We also used the mixing model and Monte Carlo method to estimate the mean flux-

273   weighted freshwater δ^2H-CH_4 and δ^{13}C-CH_4, using only the inputs for freshwater environments (Wetlands, Inland

274   Waters, and Rice Cultivation) from Table 1 (See Sect. 3.5)

275   **3 Results and Discussion**

276   **3.1 Dataset distribution**

277   The dataset is primarily concentrated in the northern hemisphere (Fig. 1A), but is distributed across a wide range

278   of latitudes between 3ºS to 73ºN (Fig. 1C). The majority of sampled sites are from North America (Fig. 1B), but there are

279 numerous sites from Eurasia. A much smaller number of sites are from South America and Africa. We define three

280 latitudinal bands for describing geographic trends: low latitudes (3ºS to 30ºN); mid-latitudes (30º to 60ºN); and high-

281 latitudes; (60º to 90ºN). This definition was used primarily because it corresponds with a commonly applied geographic

282 classification of CH_4 fluxes (Saunois et al., 2020).

283

Figure 1: Distribution of sites shown; A) on a global map, with site mean CH_4-δ^2H values indicated in relation to a color bar. Sites with and without measured δ^2H-H_2O are differentiated; B) on a map of North America; and C) as a histogram of sites by latitude, differentiated between wetlands and inland waters. Dashed lines in (C) indicate divisions between low-latitude, mid-latitude, and high-latitude sites.

288 74 of 129 sites are classified as inland waters, primarily lakes (n = 66), with a smaller number from rivers (n =

289 8). To our knowledge, all of the inland water sites are natural ecosystems and do not include reservoirs. 55 sites are

11

290   classified as wetlands, including 16 bogs, 14 swamps and marshes, 12 fens, and 8 rice paddies. For the majority of sites

291   (n = 84) gas samples were measured, whereas studies at 36 sites measured dissolved CH_4 or diffusive fluxes.

3.2 Use of δ^2H_p as an estimator for freshwater δ^2H-H_2O

293   As discussed in Sect. 2.2.3, we regressed annual and growing season δ^2H_p against measured δ^2H-H_2O to

294   determine which is a better estimator for sites where δ^2H-H_2O is not measured. We performed this analysis separately for

295   wetland and inland water environments because these broad environmental categories have distinct hydrological

296   characteristics. For all regression analyses we found strong correlations, with R^2 values between 0.82 to 0.88 (Fig. 2). For

297   wetlands, regression using annual δ^2H_p produces a slightly better fit, and also produces a slope within error of 1 (Fig 2A),

298   suggesting that variation in annual δ^2H_p scales proportionately with variation in measured δ^2H-H_2O. However, the

299   intercept of this relationship was significantly greater than 0 (19±9 ‰). We interpret this intercept as indicating that

300   evaporative isotopic enrichment is generally important in controlling δ^2H-H_2O in wetlands. A slope slightly greater than

301   1 is also consistent with evaporative enrichment, since greater evaporation rates would be expected in low-latitude

302   environments with higher δ^2H-H_2O. These results are consistent with detailed studies of wetland isotope hydrology that

303   indicate a major contribution from groundwater, with highly dampened seasonal variability relative to precipitation, but

304   also indicate evaporative enrichment of water isotopes in shallow soil water (Sprenger et al., 2017; David et al., 2018).

305   For inland waters, regression with growing season δ^2H_p produces a relationship that is within error of the 1:1

306   line (Fig. 2C), in contrast to annual δ^2H_p, which produces a flatter slope (Fig. 2D). We infer that seasonal differences in

307   δ^2H_p are important in determining δ^2H-H_2O in the inland water environments analyzed, especially at high latitudes,

308   implying that these environments generally have water residence times on subannual timescales. This finding is generally

309   consistent with evidence for seasonal variation in lake water isotopic compositions that is dependent on lake water

310   residence times (Tyler et al., 2007; Jonsson et al., 2009). Lake water residence times vary widely, primarily as a function

311   of lake size, but isotopic data implies that small lakes have water residence times of less than a year (Brooks et al., 2014),

312   resulting in seasonal isotopic variability (Jonsson et al., 2009). Isotopic enrichment of lake water is highly variable, but is

313   typically minor in humid and high-latitude regions (Jonsson et al., 2009; Brooks et al., 2014), which characterizes most

314   of our study sites.

315   Based on these results we, combine measured and estimated δ^2H-H_2O to determine a 'best-estimate' value for

316   each site, an approach similar to that of Waldron et al. (1999a). For sites with measured δ^2H-H_2O values we use that

317   value. For inland water sites without measured δ^2H-H_2O we use modeled growing season δ^2H_p since the regression of

318   this against measured δ^2H-H_2O is indistinguishable from the 1:1 line (Fig. 2D). For wetland sites without measured δ^2H-

319   H_2O we estimate δ^2H-H_2O using the regression relationship with annual precipitation δ^2H-H_2O shown in Fig. 2A. The

320   root mean square errors (RMSE) of these relationships (16‰ for wetlands, 22‰ for inland waters) provide an estimate of

the uncertainty associated with estimating δ^2H-H_2O using δ^2H_p. Given the uncertainty associated with estimating δ^2H-H_2O using δ^2H_p, for all analyses presented below that depend on δ^2H-H_2O values we also analyse the dataset only including sites with measured δ^2H-H_2O.
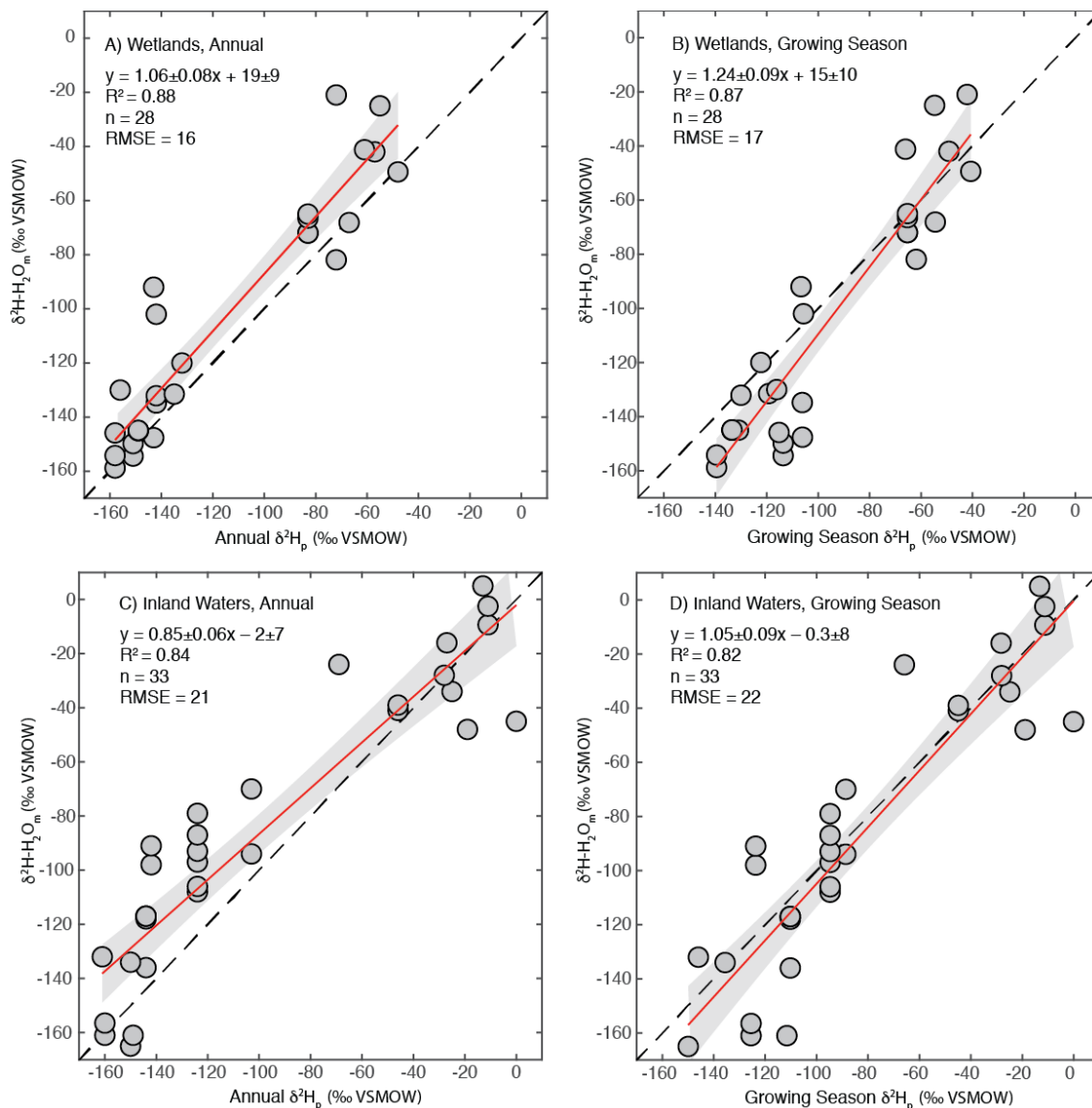

Figure 2: Scatter plots of annual or growing season δ^2H_p vs. measured δ^2H-H_2O for wetland (A,B) and inland water (C,D) sites. The red lines indicates the best fit, with a 95% confidence interval (gray envelopes), and the dashed black lines are the 1:1 relationship.

3.3 Relationship between δ^2H-H$_2$O and δ^2H-CH$_4$

We carried out regression analyses of δ^2H-H$_2$O vs. δ^2H-CH$_4$, both using 'best-estimate' δ^2H-H$_2$O as described in sect. 3.2 (Fig. 3A), and only including sites with measured δ^2H-H$_2$O (Fig. 3B). In addition we analysed the relationship for all sites using annual (Fig. 3C) and growing season (Fig. 3D) δ^2H$_p$. Identifying the relationship between modelled δ^2H$_p$ and δ^2H-CH$_4$ is of value because this could be used to create gridded global predictions of δ^2H-CH$_4$ based on gridded datasets of δ^2H$_p$ (Bowen and Revenaugh, 2003), as well as to predict the distribution of δ^2H-CH$_4$ under past and future global climates using isotope enabled Earth system models (Zhu et al., 2017).

δ^2H-CH$_4$ is significantly positively correlated with δ^2H-H$_2$O when using all four methods of estimating δ^2H-H$_2$O (Fig. 3, Supplemental Table 2). This is the case when analysing all sites together, as well as when analysing wetlands and inland waters separately (Supplemental Table 2, Fig. 4). There is no significant difference in regression relationships, based on analysis of covariance, when δ^2H-CH$_4$ is regressed against best-estimate δ^2H-H$_2$O, measured δ^2H-H$_2$O, or modelled δ^2H$_p$, nor is there a major difference in R^2 values or RMSE (Supplemental Table S2). Regression with wetland sites consistently results in a higher R^2 values and lower RMSE than regression with inland water sites.

Given the similar results when regressing with estimated or measured δ^2H-H$_2$O, we infer that using either the 'best-estimate' δ^2H-H$_2$O or modelled δ^2H$_p$, instead of measured δ^2H-H$_2$O, to predict δ^2H-CH$_4$ does not result in substantial additional error. This implies that isotope-enabled Earth Systems models (ESMs) could be used to predict the distribution of freshwater δ^2H-CH$_4$ under past and future climates based on modeled δ^2H$_p$, although the substantial scatter in Figures 3C and D should be taken into account. The southern hemisphere is highly underrepresented in the δ^2H-CH$_4$ dataset. However, the mechanisms linking δ^2H-CH$_4$ with δ^2H-H$_2$O should not differ in the southern hemisphere, and we argue that the relationships observed in this study are suitable to predict southern hemisphere freshwater δ^2H-CH$_4$. The choice of predicting δ^2H-CH$_4$ using growing-season vs. annual precipitation δ^2H$_p$ could be important, with steeper slopes overall when regressing against growing season δ^2H$_p$. Based on our analysis in sect. 3.2, we suggest that annual δ^2H$_p$ may be more appropriate for estimating wetland δ^2H-CH$_4$, while growing season δ^2H$_p$ may be more appropriate for estimating inland water δ^2H-CH$_4$. Forthcoming research will combine gridded datasets of wetland distribution (Ganesan et al., 2018), modeled annual δ^2H$_p$ (Bowen and Revenaugh, 2003), and the regression relationships from this study to predict spatially-resolved wetland δ^2H-CH$_4$ at a global scale (Stell et al., in press).
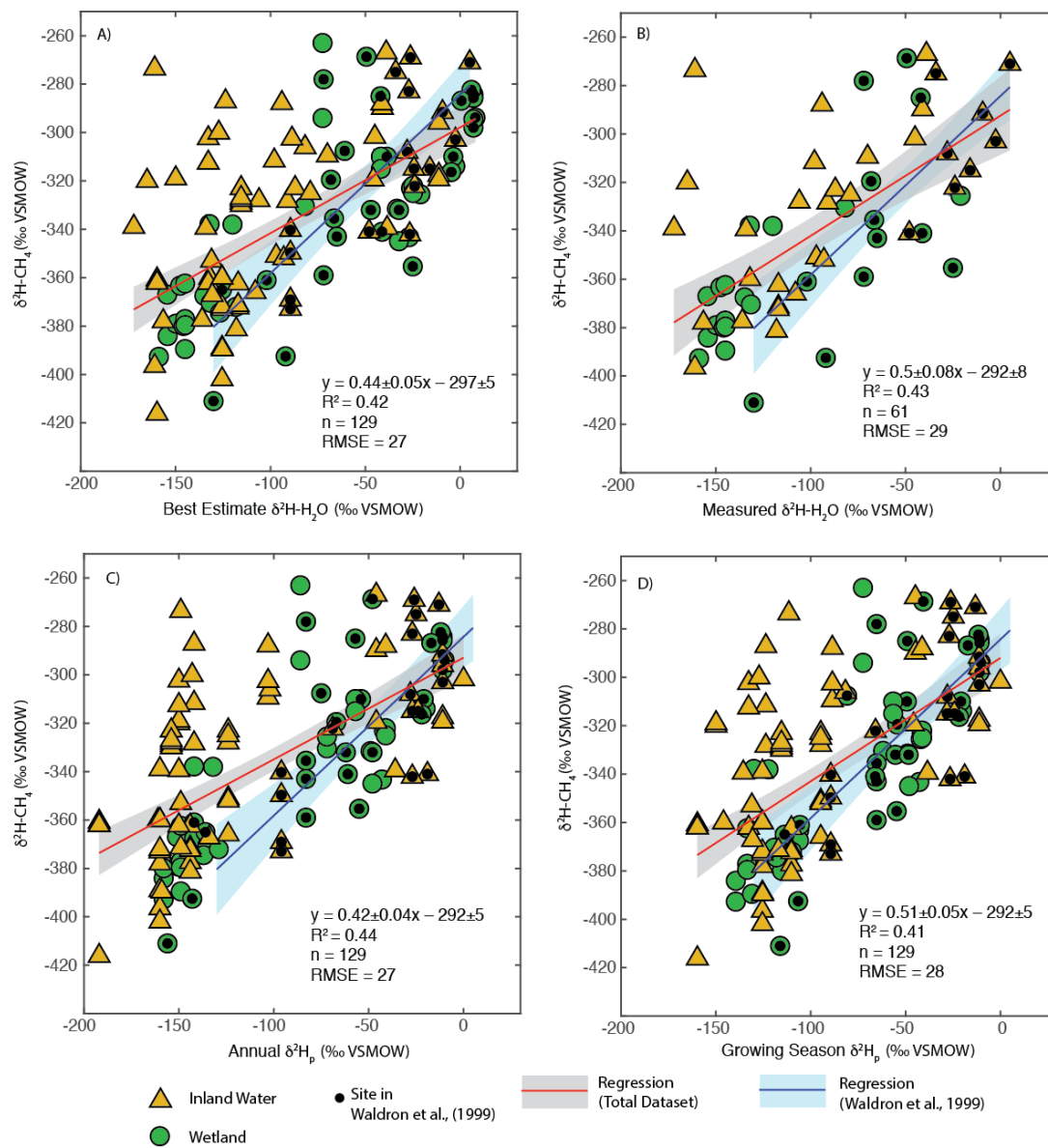
14

356

Figure 3: Scatter plots of δ^2H-CH$_4$ vs. (A) best-estimate δ^2H-H$_2$O; (B) measured δ^2H-H$_2$O; (C) annual δ^2H$_p$; and (D) growing season δ^2H$_p$. Sites that were included in the analysis of Waldron et al. (1999a) are indicated. The regression relationship for the total dataset in each plot is shown by the red line, with its 95% confidence interval (grey envelope). The regression relationship and confidence interval for the dataset of Waldron et al., (1999a) is shown in blue. Uncertainties for reported regression relationships are standard errors.

362   Overall, our results are broadly consistent with those of Waldron et al., (1999a), and confirm the finding of that

363 study that δ^2H-H$_2$O is the predominant predictor of global variation in δ^2H-CH$_4$. All of the regression slopes produced

364 using our dataset are flatter than the regression relationship found by Waldron et al. (1999a) using a smaller dataset

365 (0.68±0.1), although the slopes are not significantly different based on analysis of covariance. Based on this result we

15

366 infer that the true global relationship is likely flatter than that estimated by Waldron et al. (1999a). The difference
367 between the regression relationships reported here and that of Waldron et al. (1999a) is largely a result of a much greater
368 number of samples from the high latitudes (Fig. 1C), where δ^2H-H_2O values are typically lower. The small number of
369 high-latitude sites sampled by Waldron et al. (1999a) are skewed towards the low end of the high-latitude δ^2H-CH_4 data
370 from this study (Fig. 3). A similarly flatter slope (0.54±0.05) was found by Chanton et al. (2006) when combining a
371 dataset of δ^2H-CH_4 from Alaskan wetlands, which are included in this study, with the dataset of Waldron et al. (1999a).
372 Based on the range of R^2 values shown in Figure 3, we estimate that δ^2H-H_2O explains approximately 42% of variability
373 in δ^2H-CH_4, implying substantial residual variability, with greater residual variability for inland water sites than for
374 wetlands (Supplemental Table 2).

375   Given that δ^2H-H_2O is strongly influenced by latitude we examined whether δ^2H-CH_4 is also significantly
376 correlated with latitude. There is indeed a significant, negative relationship between latitude and δ^2H-CH_4, indicating an
377 approximate decrease of 0.9‰/° latitude (Fig. 4). The slope is significantly flatter than that for latitude vs. δ^2H-H_2O in
378 this dataset (-2 ‰/° latitude), which is consistent with the inferred slope for δ^2H-H_2O vs. δ^2H-CH_4 (0.44 to 0.5). There is
379 greater scatter in δ^2H-CH_4 at higher latitudes, especially for inland waters, but it is unclear if this is simply a result of a
380 larger sample set or of differences in the underlying processes controlling δ^2H-CH_4. We discuss latitudinal differences in
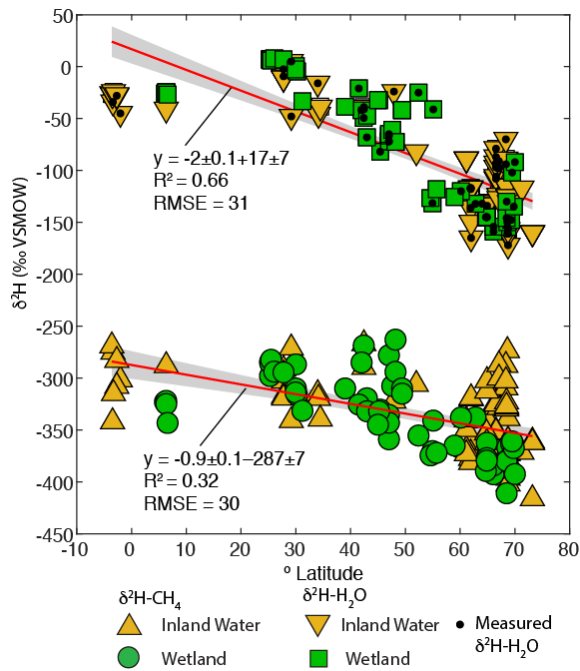381 δ^2H-CH_4 in further detail in Sect. 3.5

382

383 **Figure 4: Scatter plots of δ^2H-CH_4 and best-estimate δ^2H-H_2O, vs. latitude (ºN). Sites with measured δ^2H-H_2O are indicated.**
384 **Envelopes indicate 95% confidence intervals for regression lines.**

16

3.3.1 Comparison of δ^2H-H$_2$O vs δ^2H-CH$_4$ relationships between environmental and experimental studies

To further understand the processes controlling the observed freshwater δ^2H-H$_2$O vs. δ^2H-CH$_4$ relationships we compared them to results from pure culture and incubation experiments across a wide range of δ^2H-H$_2$O values (Fig. 5), focusing on regression against best-estimate δ^2H-H$_2$O. The regression slopes for both wetlands and inland waters (0.5 and 0.42) are within error of the 'in-vitro' relationship compiled by Waldron et al. (1999a) (0.44), based on laboratory incubations from three separate studies (Schoell, 1980;Sugimoto and Wada, 1995;Waldron et al., 1998). The intercept for the wetland and inland water regressions is higher than that for the 'in-vitro' relationship, although only the difference with inland waters is significant. In contrast, the regression slope for pure-culture acetoclastic methanogenesis experiments is much flatter (0.18 to 0.2) (Valentine et al., 2004b;Gruen et al., 2018), consistent with the prediction that one hydrogen atom is exchanged between water and the acetate methyl group during CH$_4$ formation (Pine and Barker, 1956;Whiticar, 1999). The large difference in intercept between the two acetate pure culture datasets is likely a function of differences in the δ^2H of acetate between the experiments, but could also be influenced by differences in kinetic isotope effects (Valentine et al., 2004b).

Pure culture hydrogenotrophic methanogenesis experiments (Gruen et al., 2018) yield a regression slope that is consistent with a constant α_H value, although α_H can clearly vary depending on experimental or environmental conditions (Valentine et al., 2004b;Stolper et al., 2015;Douglas et al., 2016). The wetland, inland water, and 'in-vitro' regression relationships are not consistent with a constant value of α_H (Fig. 5). Our comparison supports previous inferences that the in-vitro line of Waldron et al., (1999a) provides a good estimate of the slope of environmental δ^2H-H$_2$O vs. δ^2H-CH$_4$ relationships. This slope is likely controlled by the relative proportion of acetoclastic and hydrogenotrophic methanogenesis, the net kinetic isotope effect associated with these two methanogenic pathways, and variance in δ^2H of acetate (Waldron et al., 1998;Waldron et al., 1999a;Valentine et al., 2004a), but the relative importance of these variables remains uncertain.

In particular, the δ^2H of acetate methyl hydrogen is probably influenced by environmental δ^2H-H$_2$O, and therefore likely varies geographically as a function of δ^2H$_p$, as originally hypothesized by Waldron et al. (1999a). To our knowledge there are no measurements of acetate or acetate-methyl δ^2H from natural environments with which to test this hypothesis. In general, variability in the δ^2H of environmental organic molecules in lake sediments and wetlands, including fatty acids and cellulose, is largely controlled by δ^2H-H$_2$O (Huang et al., 2002;Sachse et al., 2012;Mora and Zanazzi, 2017), albeit with widely varying fractionation factors. The δ^2H of methoxyl groups in plants has also been shown to vary as a function of δ^2H-H$_2$O (Vigano et al., 2010). Furthermore, culture experiments with acetogenic bacteria imply that there is rapid isotopic exchange between H$_2$ and H$_2$O during chemoautotrophic acetogenesis (Valentine et al., 2004a), implying that the δ^2H of chemoautotrophic acetate is also partially controlled by environmental δ^2H-H$_2$O. Incubation experiments, such as those included in the 'in-vitro line' (Schoell, 1980;Sugimoto and Wada, 1995;Waldron

17

et al., 1998), probably contain acetate-δ^2H that varies as a function of ambient δ^2H-H_2O, given that the acetate in these incubation experiments was actively produced by fermentation and/or acetogenesis during the course of the experiment. This differs from pure cultures of methanogens, where acetate is provided in the culture medium and therefore does not vary in its δ^2H value (Valentine et al., 2004b; Gruen et al., 2018).
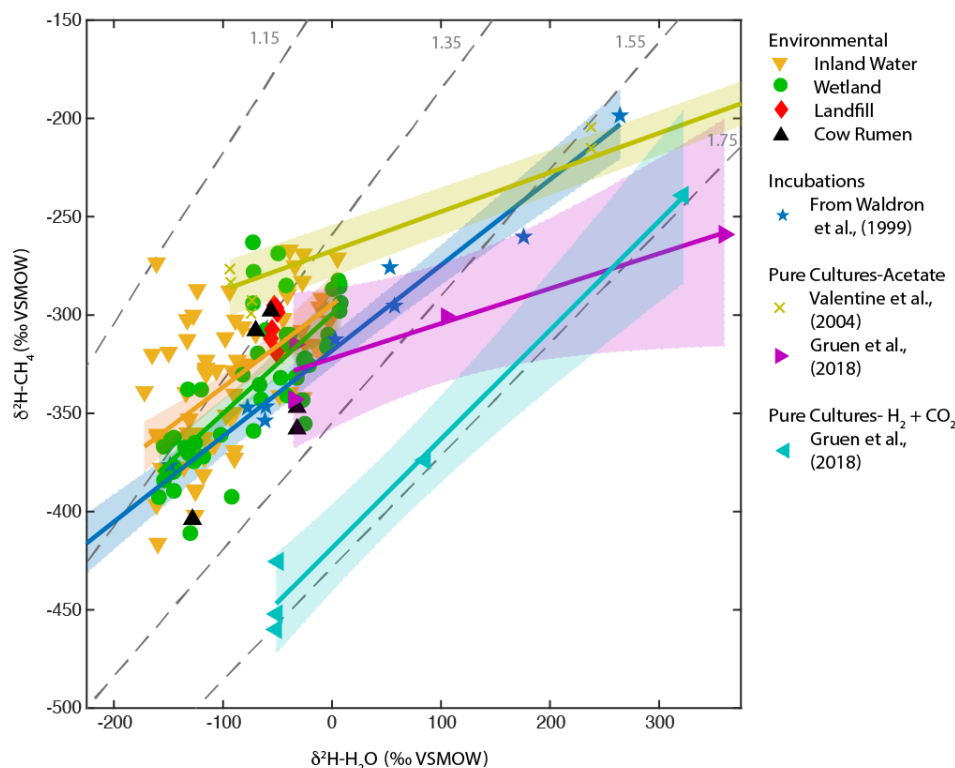

Figure 5: Scatter plots of δ^2H-CH_4 vs. δ^2H-H_2O for wetlands, inland waters, landfills, and cow rumen, compared with incubation and pure-culture experiments. Regression lines and confidence intervals corresponding to each dataset (except landfills and cow rumen) are shown. Dashed gray lines indicate constant values of α_H. Regression line statistics are listed in Supplemental Table S2. Plotted δ^2H-H_2O values are 'best-estimate' values for wetlands and inland waters, measured values for culture experiments, and a combination of measured values and annual δ^2H_p for landfills and cow rumen (See supplemental Table S3 for more details).

3.4 Relationship of δ^2H-CH_4 with δ^{13}C-CH_4, δ^{13}C-CO_2, and α_C

As shown in Fig. 3, there is a large amount of residual variability in δ^2H-CH_4 that is not explained by δ^2H-H_2O. Several biogeochemical variables have been proposed to influence freshwater δ^2H-CH_4 independently of δ^2H-H_2O, including the predominant biochemical pathway of methanogenesis (Whiticar et al., 1986;Whiticar, 1999;Chanton et al., 2006), the extent of methane oxidation (Happell et al., 1994;Waldron et al., 1999a;Whiticar, 1999;Cadieux et al., 2016), isotopic fractionation resulting from diffusive gas transport (Waldron et al., 1999a;Chanton, 2005), and differences in the thermodynamic favorability or reversibility of methanogenesis (Valentine et al., 2004b;Stolper et al., 2015;Douglas et al.,

18

436   2016). These variables are also predicted to cause differences in $\delta^{13}C$-CH_4, $\delta^{13}C$-CO_2, and α_C. Therefore, we analysed co-

437   variation between δ^2H-$CH_{4,W0}$ (see definition in Sect. 2.2.3) and $\delta^{13}C$-CH_4, $\delta^{13}C$-CO_2, and α_C to see if it could partially

438   explain the residual variability in δ^2H-CH_4 (Fig. 6).

439   In order to facilitate interpretation of isotopic co-variation, we estimated approximate vectors of predicted

440   isotopic co-variation for the four variables being considered (Fig. 6). We emphasize that these vectors are uncertain, and

441   while they can be considered indicators for the sign of the slope of co-variation and the relative magnitude of expected

442   isotopic variability, they are not precise representations of the slope or intercept of isotopic co-variation. In reality,

443   isotopic co-variance associated with these processes likely varies depending on specific environmental conditions,

444   although the sign of co-variance should be consistent. The starting point for the vectors is arbitrarily set to typical

445   isotopic values for inferred acetoclastic methanogenesis in freshwater systems (Whiticar, 1999). We based the vectors for

446   differences in the dominant methanogenic pathway and methane oxidation on Figures 8, 5, and 10 in Whiticar (1999).

447   These figures are widely applied to interpret environmental isotopic data related to CH_4 cycling. However, we note that

448   both environmental and experimental research has questioned whether differences in the dominant methanogenic

449   pathway has an influence on δ^2H-CH_4 (Waldron et al., 1998;Waldron et al., 1999a). Differences in δ^2H-CH_4 between

450   hydrogenotrophic and acetoclastic methanogenesis are likely highly dependent on both the δ^2H of acetate and the carbon

451   and hydrogen kinetic isotope effects for both methanogenic pathways, both of which are poorly constrained in natural

452   environments and are likely to vary between sites (see Sect. 3.3.1). We did not differentiate between anaerobic and

453   aerobic methane oxidation, and the vectors shown are similar to experimental results for aerobic methane oxidation

454   (Wang et al., 2016).

455   The vector for isotopic fractionation related to gas-phase diffusion is based on the calculations of Chanton

456   (2005), and indicates isotopic change for residual gas following a diffusive loss. Gas-liquid diffusion is predicted to have

457   a much smaller isotopic effect (Chanton, 2005). The vector for differences in enzymatic reversibility are based on

458   experiments where CH_4 and CO_2 isotopic compositions were measured together with changes in methane production rate

459   or Gibbs free energy (Valentine et al., 2004b;Penning et al., 2005). We note that these studies did not measure δ^2H-CH_4

460   in the same experiments as $\delta^{13}C$-CH_4 or $\delta^{13}C$-CO_2, implying large uncertainty in the co-variance vectors. More detail on

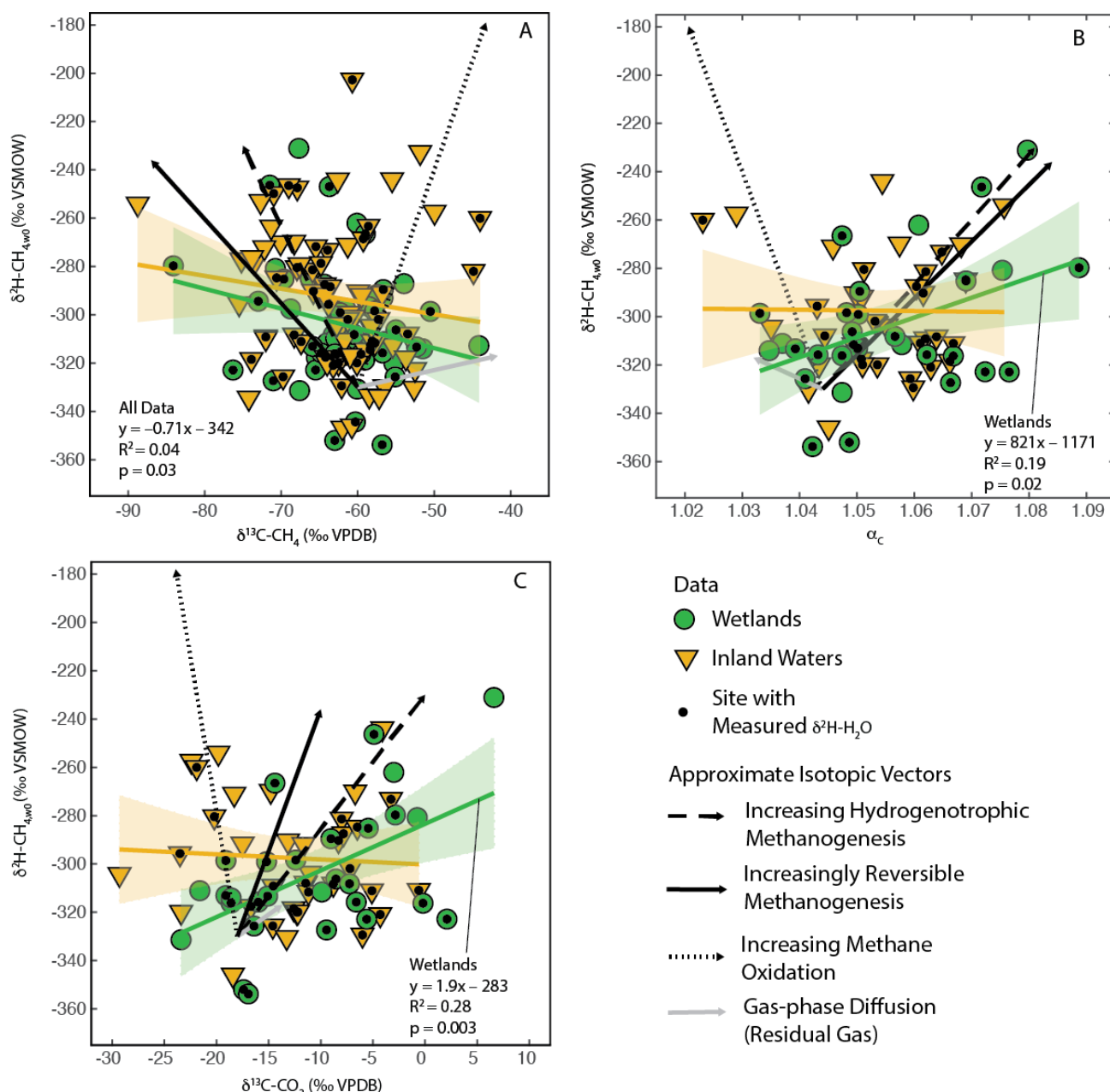461   the estimated vectors is provided in the Supplementary Text.

19

Figure 6: Scatter plots of δ^2H-$CH_{4,w0}$ vs. (A) $\delta^{13}C$-CH_4, (B) α_c, and (C) $\delta^{13}C$-CO_2. Approximate vectors for isotopic co-variation related to four biogeochemical variables are shown. See details in Sect. 3.4 and the supplemental text. Regression relationships are shown for wetland and inland water sites, with envelopes indicating 95% confidence intervals. Regression statistics are shown here for relationships with significant correlations ($p < 0.05$). All regression statistics are detailed in Supplemental Table S4.

468   We observe significant positive correlations between $\delta^2H\text{-}CH_{4,W0}$, calculated using best estimate $\delta^2H\text{-}H_2O$, and
469   both $\delta^{13}C\text{-}CO_2$, and α_C for wetland sites (Fig. 6B,C; Supplemental Table S4). We do not observe a significant correlation
470   between these variables for inland water sites or for the dataset as a whole. We also observe a weak but significant
471   negative correlation between $\delta^2H\text{-}CH_{4,W0}$ and $\delta^{13}C\text{-}CH_4$ for all sites, but not for data disaggregated into wetlands and
472   inland water categories (Fig. 6A). The correlations shown in Figure 6 should be interpreted with caution, since repeating
473   this analysis only using sites with measured $\delta^2H\text{-}H_2O$ does not result in any significant correlations (Supplemental Table
474   S4). It is unclear whether this different result when using best-estimate or measured $\delta^2H\text{-}H_2O$ represents a bias related to
475   estimating $\delta^2H\text{-}H_2O$ using δ^2H_p, or is an effect of the much smaller sample size for sites with $\delta^2H\text{-}H_2O$ measurements. If
476   accurate, the observed significant positive correlations in Figures 6B and C suggest that residual variability in $\delta^2H\text{-}CH_4$
477   in wetlands is more strongly controlled by biogeochemical variables related to methanogenesis, namely differences in
478   methanogenic pathway or thermodynamic favorability, than post-production processes such as diffusive transport and
479   CH_4 oxidation. For inland water sites our analysis suggests that no single biogeochemical variable has clear effect in
480   controlling residual variability in $\delta^2H\text{-}CH_4$.

481   Overall, our results are not consistent with arguments that residual variability in freshwater $\delta^2H\text{-}CH_4$ is
482   dominantly controlled by either differences in methanogenic pathway (Chanton et al., 2006), or post-production
483   processes (Waldron et al., 1999a). Instead they highlight the combined influence of a complex set of variables and
484   processes that are difficult to disentangle on an inter-site basis using $\delta^{13}C$ measurements alone. It is also important to
485   note the likely importance of variables that could influence $\delta^{13}C\text{-}CH_4$ or $\delta^{13}C\text{-}CO_2$ but not necessarily affect $\delta^2H\text{-}CH_4$,
486   including variance in the $\delta^{13}C$ of soil or sediment organic matter (Conrad et al., 2011;Ganesan et al., 2018), diverse
487   metabolic and environmental sources and sinks of CO_2 in aquatic environments, and Rayleigh fractionation associated
488   with CH_4 carbon substrate depletion (Whiticar, 1999). Finally, the possible role of other carbon substrates, such as
489   methanol, in CH_4 production could be important in controlling isotopic co-variation. Culture experiments suggest that
490   CH_4 produced from methanol has low $\delta^{13}C$ and δ^2H values relative to other pathways (Krzycki et al., 1987;Penger et al.,
491   2012;Gruen et al., 2018), although the importance of this difference in environmental CH_4 is unclear.

492   Further research examining intra-site isotopic co-variation, which largely avoids complications associated with
493   estimating $\delta^2H\text{-}H_2O$, would help to more clearly resolve the relative importance of these processes, and how they vary
494   between environments. Expanded research using methyl fluoride to inhibit acetoclastic methanogenesis (Penning et al.,
495   2005;Penning and Conrad, 2007;Conrad et al., 2011), with a particular focus on $\delta^2H\text{-}CH_4$ measurements, would also help
496   to clarify the importance of methanogenic pathway on isotopic co-variation. Finally, an expanded application of
497   measurements of clumped isotopes, which have distinctive patterns of variation related to these processes (Douglas et al.,

498   2016; Douglas et al., 2017; Young et al., 2017; Douglas et al., 2020), would also be of value in determining their relative

499   importance in controlling δ^2H-CH$_4$ values in freshwater environments.

3.5 Differences in δ^2H-CH$_4$ and δ^{13}C-CH$_4$ by latitude

501   When analysing all sites together we found a significant difference in the distribution of δ^2H-CH$_4$ between high-

502   latitude sites (median: -351‰) and both low (median: -298‰) and mid-latitude sites (median: -320 ‰) (Fig. 7A).

503   However, we did not find a significant difference in the distribution of low- and mid-latitude sites. Similar differences

504   were found when the data were disaggregated into wetland and inland water sites. We also found that the distribution of

505   δ^{13}C-CH$_4$ for low latitude sites (median: -61.6‰) was significantly higher than for high latitude sites (median: –63.0‰),

506   but that mid-latitude sites (median: -60.3‰) were not significantly different from the other two latitudinal zones (Fig.

507   7B). The observed difference by latitudinal zone in δ^{13}C-CH$_4$ appears to be driven primarily by latitudinal differences

508   between inland water sites, where a similar pattern is found. In wetland sites we found no significant differences in the
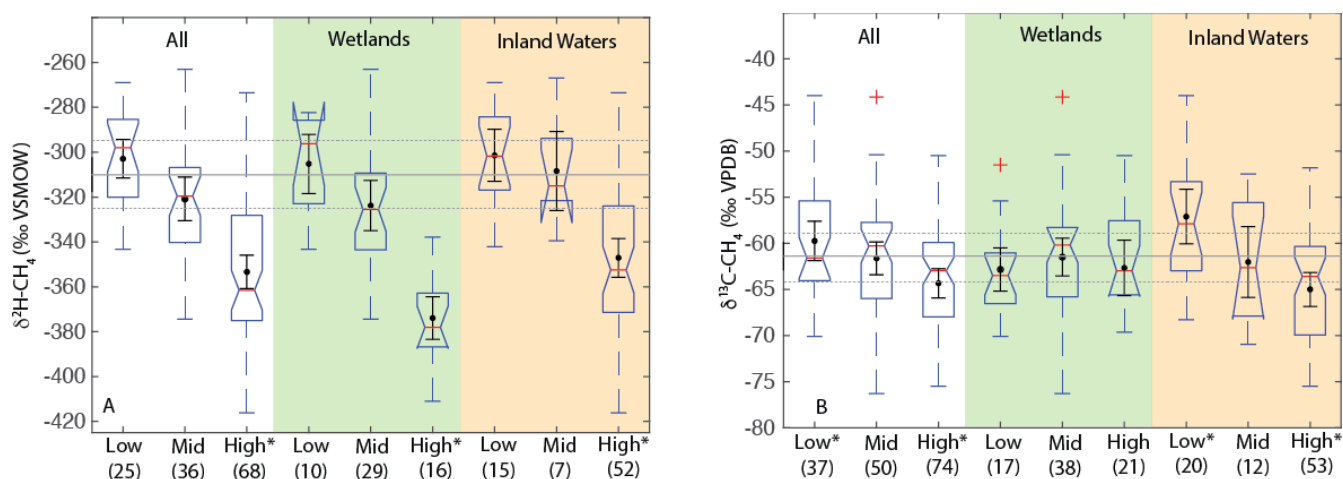
509   distribution of δ^{13}C-CH$_4$ by latitude.

510

Figure 7: Boxplots of (A) δ^2H-CH$_4$ and (B) δ^{13}C-CH$_4$ for sites differentiated by latitude, for all data, wetlands, and inland waters. Numbers in parentheses indicate the number of sites for each category. Red lines indicate medians, boxes indicate 25th and 75th percentiles, whiskers indicate 95th and 5th percentiles, and outliers are shown as red crosses. Notches indicate the 95% confidence intervals of the median value; where notches overlap the edges of the box this indicates the median confidence interval exceeds the 75th or 25th percentile. Black points and error bars indicate the category mean and 95% confidence interval of the mean. Gray lines indicate the estimated flux-weighted mean values for global freshwater CH$_4$, and dashed lines indicate the 95% confidence interval of this value. Asterisks in (A) indicate that high-latitude sites have significantly different distributions from other latitudinal bands. Asterisks in (B) indicate groups that have significantly different distributions from one another, within a specific environmental category. Two extremely low outliers (<-80‰; high latitude wetland and inland water) are not shown in (B).

521   Estimates of flux-weighted mean freshwater δ^2H-CH$_4$ and δ^{13}C-CH$_4$, calculated using the Monte Carlo approach

522   described in Sect. 2.4, are -310±15‰ (Fig. 7A) and -61.5±3‰ (Fig. 7B) respectively. Flux weighted mean values for

523   natural wetlands (not including inland waters or rice paddies) are -310±25‰ for δ^2H-CH$_4$ and -63.9±3.3‰ for δ^{13}C-CH$_4$.

22

524   Flux weighted mean values for inland waters are -309±31‰ for δ^2H-CH$_4$ and -60±5.7‰ for δ^{13}C-CH$_4$. As discussed in

525   Sect. 2.4 there are limited data in our dataset or that of Sherwood et al., (2017) from C$_4$ plant dominated wetlands, and

526   therefore our low-latitude and flux-weighted mean δ^{13}C-CH$_4$ values for wetlands are probably biased towards low values.

527   Differences in δ^2H-CH$_4$ by latitude has the potential to aid in geographic discrimination of freshwater methane

528   sources, both because it is based on a clear mechanistic linkage with δ^2H-H$_2$O (Figs. 3 and 4), and because geographic

529   variation in δ^2H-H$_2$O is relatively well understood (Bowen and Revenaugh, 2003;Bowen et al., 2005). However, recent

530   studies of atmospheric δ^2H-CH$_4$ variation have typically not accounted for geographic variation in source signals. As an

531   example, Rice et al., (2016) apply a constant δ^2H-CH$_4$ of -322‰ for both low-latitude (0-30º N) and high latitude (30-

532   90º N) wetland emissions. Based on our dataset this estimate is an inaccurate representation of wetland δ^2H-CH$_4$ for

533   either 0-30º N (mean: -305±13‰) or 30-90º N (mean: -345±11‰). Studies of ice core measurements have more

534   frequently differentiated freshwater δ^2H-CH$_4$ values as a function of latitude. For example, Bock et al., (2010)

535   differentiated δ^2H-CH$_4$ between tropical (-320‰) and boreal (-370‰) wetlands. This tropical wetland signature is

536   significantly lower than our estimate of low-latitude wetland δ^2H-CH$_4$, although the boreal wetland signature is similar to

537   our mean value for high-latitude wetlands (-374±10‰). Overall, our results imply that accounting for latitudinal variation

538   in freshwater δ^2H-CH$_4$, along with accurate latitudinal flux estimates, is important for developing accurate estimates of

539   global freshwater δ^2H-CH$_4$ source signatures.

540   Our analysis indicates significant differences in the distribution of freshwater δ^{13}C-CH$_4$ between the low- and

541   high-latitudes, but mid-latitude sites cannot be differentiated. Furthermore our results do not indicate significant

542   latitudinal differences in δ^{13}C-CH$_4$ for wetland sites in particular.. This is in contrast to previous studies that have

543   inferred significant differences in wetland δ^{13}C-CH$_4$ by latitude (Bock et al., 2010;Rice et al., 2016;Ganesan et al., 2018).

544   An important caveat is that we have not analyzed a comprehensive dataset of freshwater δ^{13}C-CH$_4$, for which there are

545   much more published data than for δ^2H-CH$_4$, although our analysis does comprise the largest dataset of freshwater δ^{13}C-

546   CH$_4$ compiled to date (See Sect. 2.3). In addition, our analysis does not take into account the geographic distribution of

547   different ecosystem categories, although we do not find significant differences in δ^{13}C-CH$_4$ between ecosystem

548   categories (Fig. 8; Sect. 3.6). Low-latitude ecosystems dominated by C$_4$ plants are underrepresented both in our dataset

549   and that of Sherwood et al., (2017), and accounting for this would likely lead to a more enriched low-latitude wetland

550   δ^{13}C-CH$_4$. In contrast, high-latitude ecosystems, including bogs, are relatively well represented in these datasets (Fig. 8),

551   and we suggest that inferences of especially low δ^{13}C-CH$_4$ in high-latitude wetlands (Bock et al., 2010;Rice et al.,

552   2016;Ganesan et al., 2018) are not consistent with the compiled dataset of in-situ measurements. However, we note that

553   atmospheric estimates of high-latitude wetland δ^{13}C-CH$_4$ (~-68±4‰; Fisher et al., 2011) are lower than the median or

554   mean value shown in Figure 7B, and are in close agreement with the relatively low values predicted by (Ganesan et al.,

555   2018). Ombrotrophic and minerotrophic peatlands have distinctive δ^{13}C-CH$_4$ signatures (Bellisario et al., 1999;Bowes

and Hornibrook, 2006;Hornibrook, 2009), with lower signatures in ombrotrophic peatlands. We did not differentiate peatlands by trophic status, and it is possible that the dataset of high-latitude wetland in-situ measurements is biased towards minerotrophic peatlands with relatively high $\delta^{13}C$-CH_4.

Latitudinal differences in $\delta^{13}C$-CH_4 inferred by Ganesan et al. (2018) were based on two key mechanisms: (1) differences in methanogenic pathway between different types of wetlands, especially between minerotrophic fens and ombrotrophic bogs; and (2) differential inputs of organic matter from C_3 and C_4 plants. Because inferred latitudinal differences in $\delta^{13}C$-CH_4 and δ^2H-CH_4 are caused by different mechanisms, they could be highly complementary in validating estimates of freshwater emissions by latitude. It is also important to note that previous assessments of latitudinal differences in $\delta^{13}C$-CH_4 did not include inland water environments. Our analysis suggests that latitudinal variation in $\delta^{13}C$-CH_4 in inland waters may be more pronounced than in wetlands, although the mechanisms causing this difference will need to be elucidated with further study. A benefit of geographic discrimination based on δ^2H-CH_4 is that the same causal mechanism applies to all freshwater emissions, including both wetlands and inland waters.

3.5.1 Potential for geographic discrimination of other microbial methane sources based on δ^2H-CH_4

We speculate that latitudinal differences in δ^2H-CH_4 should also be observed in other fluxes of microbial methane from terrestrial environments, including enteric fermentation in livestock and wild animals, manure ponds, landfills, and termites. This is because microbial methanogenesis in all of these environments will incorporate hydrogen from environmental water, and therefore will be influenced by variation in precipitation δ^2H. There are limited data currently available to test this prediction, but δ^2H-CH_4 data from cow rumen and landfills are available with either specified locations or δ^2H-H_2O (Burke Jr, 1993;Levin et al., 1993;Liptay et al., 1998;Bilek et al., 2001;Wang et al., 2015;Teasdale et al., 2019). These data plot in a range that is consistent with the δ^2H-CH_4 vs. δ^2H-H_2O relationships for freshwater CH_4 (Fig. 5). Landfill data are only available for a very small range of estimated δ^2H-H_2O, making it impossible to assess for geographic variation currently. δ^2H-CH_4 data from cow rumen span a much wider range, and express substantial variation that is independent of δ^2H-H_2O, but largely overlap measurements from freshwater environments. Based on these limited data, variation observed in incubation studies that simulate landfill conditions (Schoell, 1980;Waldron et al., 1998), and our understanding of the influence of δ^2H-H_2O on microbial δ^2H-CH_4 (Fig. 6), we suggest that both landfill and cow rumen δ^2H-CH_4 likely vary geographically as a function of δ^2H-H_2O. If validated, this variation could also be used to distinguish these CH_4 sources geographically. More data are clearly needed to test this conjecture, and it will also be important to evaluate how closely annual or seasonal δ^2H_p corresponds to environmental δ^2H-H_2O in both landfills and cow rumen. Relatedly, the δ^2H of CH_4 emitted by biomass burning or directly by plants has also been shown to vary as a function of δ^2H-H_2O (Vigano et al., 2010;Umezawa et al., 2011).

3.6 Differences in δ^2H-CH$_4$ and δ^{13}C-CH$_4$ by ecosystem

When comparing ecosystems, we analyze δ^2H-CH$_{4,W0}$ values to account for variability related to differences in δ^2H-H$_2$O. Ecosystem types are not evenly distributed by latitude, and therefore have different distributions of δ^2H-H$_2$O values. Our analysis does not find a significant difference in the distribution of δ^2H-CH$_{4,W0}$ between ecosystems, which could be partly a result of small sample sizes for most ecosystem categories (Fig. 8). Comparing the broader categories of inland waters and wetlands, we do observe a significant difference in δ^2H-CH$_{4,W0}$ distributions, with inland waters shifted towards higher values (median: -296‰) than wetlands (median: -311‰). We repeated this analysis only including sites with measured δ^2H-H$_2$O and found the same results in terms of category differences (Supplemental Figure S1). We did not observe any significant differences in δ^{13}C-CH$_4$ distributions between ecosystems, nor was there a significant difference in δ^{13}C-CH$_4$ distributions between inland waters and wetlands.

The significant difference in the distribution of δ^2H-CH$_{4,W0}$ between inland waters and wetlands is primarily a result of the difference in δ^2H-CH$_4$ between these environments in the high latitudes (Figs. 3, 4, and 7). We suggest this difference could be related to a greater overall prevalence of CH$_4$ oxidation in inland waters. As shown in Figure 6, the lack of positive co-variation between δ^2H-CH$_{4,W0}$ and δ^{13}C-CO$_2$, and α_C could be interpreted to support a greater role for CH$_4$ oxidation to control δ^2H-CH$_{4,W0}$ in inland waters relative to wetlands, although this result requires further validation. In lakes that undergo seasonal overturning and water column oxygenation there may be a greater overall effect of CH$_4$ oxidation than there are in wetlands typically. The absence of significant differences between ecosystems in terms of δ^{13}C-CH$_4$ (Fig. 8B) is in contrast to previous studies that have suggested that fens and bogs in particular have distinctive δ^{13}C-CH$_4$ (Ganesan et al., 2018). Bogs in particular have a very wide distribution of δ^{13}C-CH$_4$ that could represent differences between minerotrophic and ombrotrophic bogs (Hornibrook, 2009), which we did not differentiate in our dataset. This result should be interpreted with caution given that our dataset is not a comprehensive compilation of published δ^{13}C-CH$_4$ data, although it is the largest compiled dataset available (Sect. 2.3). We argue that inferred differences in δ^{13}C-CH$_4$ between wetland ecosystem categories should be further verified with more comprehensive data assimilation and additional measurements.
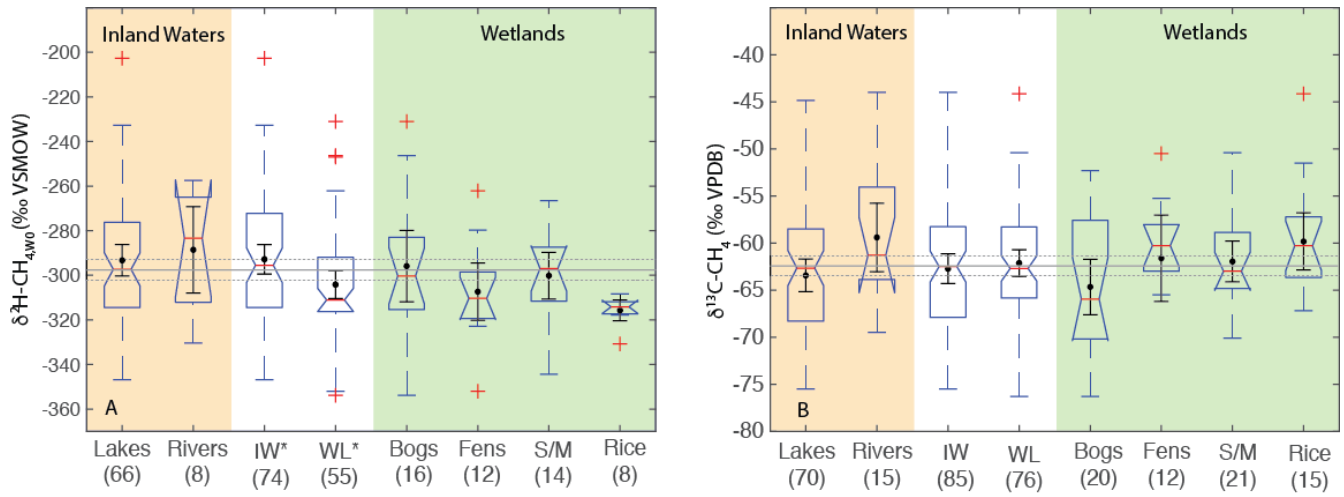
Figure 8: Boxplots of (A) δ^2H-CH$_{4,w0}$ and (B) δ^{13}C-CH$_4$ for sites differentiated by ecosystem type. **Numbers in parentheses indicate the number of sites for each category. Boxplot parameters are as in Fig. 7. Black points and error bars indicate the category mean and 95% confidence interval of the mean. Gray lines indicate the mean values across all categories and the dashed lines indicate the 95% confidence interval of this value. Two extremely low outliers (<-80‰; lake and fen) are not shown in (B). IW- Inland Waters; WL- Wetlands; S/M- Swamps and marshes. Asterisks in A indicate that inland waters and wetlands have significantly different distributions.**

3.7 Differences in δ^2H-CH$_4$ and δ^{13}C-CH$_4$ by sample type

As with comparing ecosystems, when comparing sample types we analyze δ^2H-CH$_{4,W0}$ values to normalize for variability related to differences in δ^2H-H$_2$O, since sample types are not distributed evenly by latitude. When comparing sample types, dissolved CH$_4$ samples do not have a significantly different δ^2H-CH$_{4,W0}$ distribution for the dataset as a whole, nor is there a significant difference between these groups in wetland sites (Fig. 9A). There is, however, a significant difference in inland water sites, with dissolved CH$_4$ samples having a more enriched distribution (median: -270‰) vs. gas samples (median: -302‰). We repeated this analysis only including sites with measured δ^2H-H$_2$O and found the same results in terms of category differences (Supplemental Figure S2). We did not observe a significant difference in the distribution of δ^{13}C between dissolved and gas-phase CH$_4$ samples, either for the dataset as a whole or when the dataset was disaggregated into wetlands and inland waters (Fig. 9B).

We suggest that the higher δ^2H-CH$_{4,W0}$ in dissolved vs. gas samples for inland waters could be a result of generally greater oxidation of dissolved CH$_4$ in inland water environments, potentially as a result of longer exposure to aerobic conditions in lake or river water columns. This is in contrast to wetlands, where aerobic conditions are generally limited to the uppermost layers of wetlands proximate to the water table. However, our dataset for inland water dissolved

26

631 CH$_4$ is quite small (n=9), and more data are needed to test this hypothesis. Furthermore, it is unclear why oxidation in

632 inland water dissolved CH$_4$ would be more strongly expressed in terms of δ^{2}H-CH$_{4,W0}$ (Fig. 9A) than δ^{13}C (Fig. 9B).

633   Overall, our data imply that isotopic differences between dissolved and gas phase methane are relatively minor

634 on a global basis, especially in wetlands. This result could imply that the relative balance of diffusive vs. ebullition gas

635 fluxes does not have a large effect on the isotopic composition of freshwater CH$_4$ emissions. However, our study does not

636 specifically account for isotopic fractionation occurring during diffusive or plant-mediated transport (Hornibrook, 2009),

637 and most of our dissolved sample data are of *in-situ* dissolved CH$_4$ and not diffusive fluxes. More isotopic data

638 specifically focused on diffusive methane emissions, for example using measurements of gas sampled from chambers,

639 would help to resolve this question, as would more comparisons of the isotopic composition of diffusive and ebullition
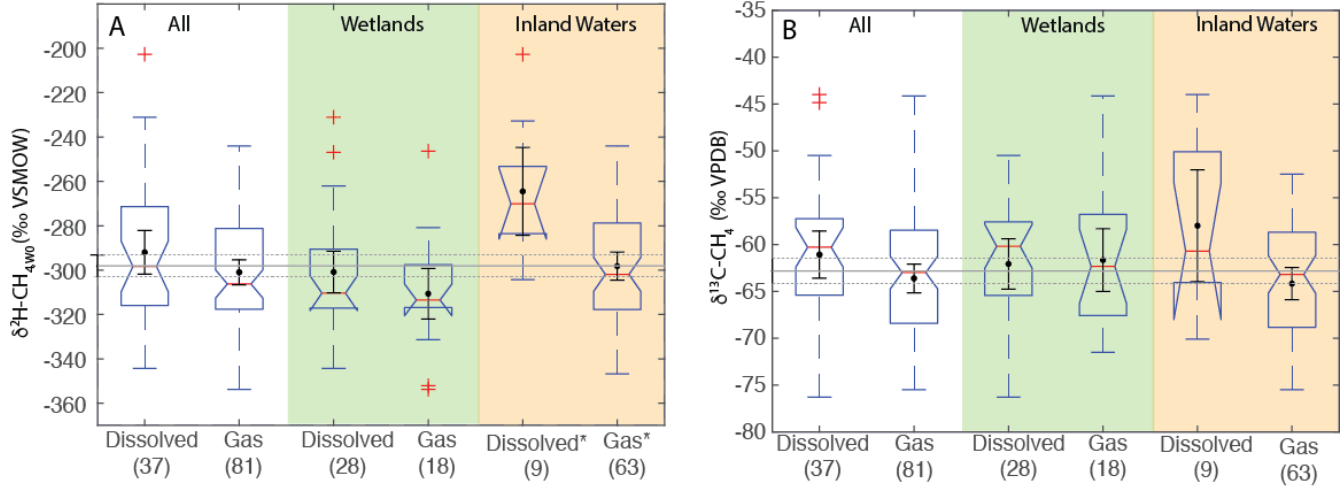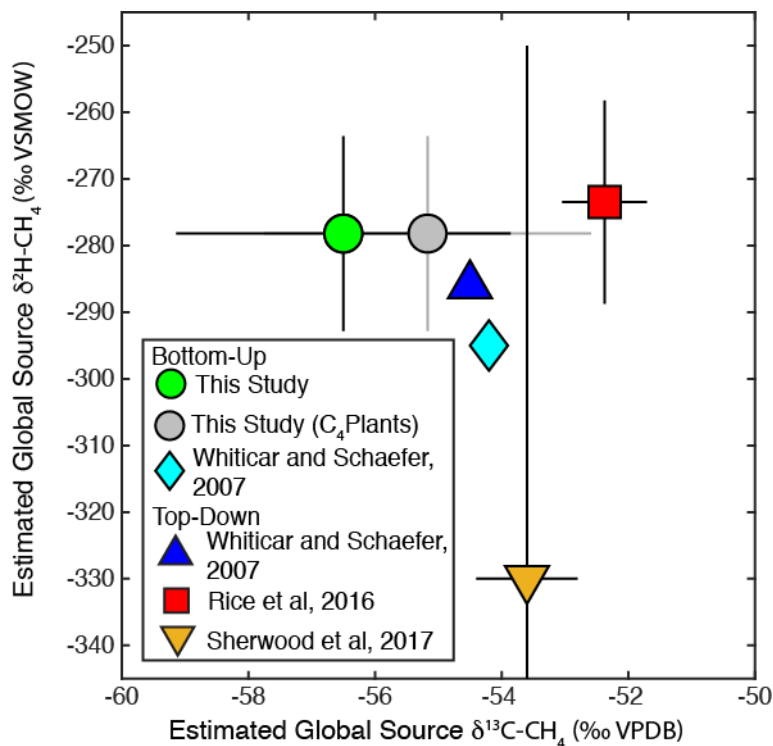
640 CH$_4$ emissions from the same ecosystem.

641

642 **Figure 9: Boxplots of (A) δ^{2}H-CH$_{4,w0}$ and (B) δ^{13}C-CH$_4$ for sites differentiated by sample type. Numbers in parentheses**

643 **indicate the number of sites for each category. Boxplot parameters are as in Fig. 7. Black points and error bars indicate the**

644 **category mean and 95% confidence interval of the mean. Gray lines indicate the mean values across all categories and the**

645 **dashed lines indicate the 95% confidence interval of this value. Two extremely low outliers (<-80‰; dissolved wetland and gas**

646 **inland water) are not shown in (B). Asterisks in A indicate that dissolved and gas-phase CH$_4$ samples from inland water sites**

647 **have significantly different distributions.**

648 **3.8 Estimates of global emissions source δ^{2}H-CH$_4$ and δ^{13}C-CH$_4$**

649 Our mixing model estimates a global source δ^{2}H-CH$_4$ of -278±15‰, and a global source δ^{13}C-CH$_4$ of -56.4±2.6‰ (Fig.

650 10). Monte Carlo sensitivity tests that only included uncertainty in either isotopic source signatures or flux estimates

651 suggest that larger uncertainty is associated with isotopic source signatures (12‰ for δ^{2}H; 2.2‰ for δ^{13}C) than with flux

652 estimates (8‰ for δ^{2}H; 1.4‰ for δ^{13}C). When correcting for wetland and biomass burning emissions from C$_4$ plant

653 ecosystems, as described in Section 2.4, our estimate of global source δ^{13}C-CH$_4$ increases to -55.2±2.6‰. Our estimate of

27

654 global source δ^2H-CH$_4$ is substantially higher than a previous bottom-up estimate using a similar approach (-295‰; Fig.

655 10) (Whiticar and Schaefer, 2007). This difference can be largely attributed to the application of more depleted δ^2H-CH$_4$

656 source signatures for tropical wetlands (-360 ‰), and to a lesser extent boreal wetlands (-380 ‰), by Whiticar and

657 Schaefer (2007).

658

Figure 10: Comparison of estimates of dual-isotope global source δ^2H-CH$_4$ and δ^{13}C-CH$_4$ from this and previous studies. Error
bars from this study indicate the 2σ standard deviation from Monte Carlo analysis. Gray dot and error bars indicate an
estimate corrected for the lack of data from wetlands and biomass burning in C$_4$ plant environments, as described in Sect. 2.4.
Error bars for Rice et al., (2016), indicate the range of values estimated in that study between 1977-2005. Error bars for
Sherwood et al., (2017) reflect the combined measurement uncertainty and uncertainty in sink fractionations reported in that
study. Whiticar and Schaefer (2007) did not provide uncertainties for their estimates.

665 Our bottom-up estimate of global source δ^2H-CH$_4$ substantially overlaps the range of top-down estimates (-258

666 to -289‰) based on atmospheric δ^2H-CH$_4$ measurements from 1977-2005 and a box model of sink fluxes and kinetic

667 isotope effects (Rice et al., 2016) (Fig. 10). It is also within error of simpler top-down estimates calculated based on

668 mean atmospheric measurements and estimates of a constant sink fractionation factor (Whiticar and Schaefer,

669 2007;Sherwood et al., 2017). Sherwood et al., (2017) estimate a very wide range of possible global source δ^2H-CH$_4$

670 values based on a relatively large atmospheric sink fractionation with large uncertainty (-235±80‰). This range overlaps

671 with our bottom up estimate, although its mid-point is substantially lower than our estimate. We argue that the box-model

672   method used to account for sink fractionations applied by Rice et al. (2016) probably provides a more accurate

673   representation of global-source isotopic composition than the other top-down estimates shown in Figure 10. The

674   estimates of Rice et al. (2016) are also supported by the results of a global inversion model. Overall, the overlap between

675   our bottom-up estimate of global source δ^2H-CH$_4$ with top-down estimates is encouraging, and suggests that the

676   estimates of emission source δ^2H-CH$_4$ signatures applied in this study are reasonably accurate. However, as discussed

677   below, there is still substantial scope to further constrain these estimates and to reduce uncertainty.

678   Our bottom-up estimate of global source δ^{13}C-CH$_4$ is lower than the other top-down and bottom-up estimates

679   shown in Figure 10. As discussed above, there is likely a bias in our freshwater CH$_4$ isotopic database in that it includes

680   very few wetland sites from C$_4$-plant dominated ecosystems. When correcting for this, as well as for CH$_4$ emissions from

681   combustion of C$_4$ plants (Fig. 10), our estimate shifts to a more enriched value that is within uncertainty of other

682   estimates. Clearly, accounting for the effect of C$_4$ plants in wetland and biomass burning CH$_4$ emissions, and potentially

683   also in enteric fermentation emissions, is important for accurate estimates of global source δ^{13}C-CH$_4$. As discussed

684   below, other sources of error in both isotopic source signatures and inventory-based flux estimates could also partially

685   account for our relatively low global source δ^{13}C-CH$_4$ estimate. For example, variation in fossil fuel isotopic signatures

686   between regions and resource types is potentially an additional source of uncertainty that is not accounted for in this

687   estimate.

688   Previous studies have argued, on the basis of comparing atmospheric measurements and emissions source δ^{13}C-

689   CH$_4$ signatures, that there are biases in global emissions inventories, specifically that fossil fuel emissions estimates are

690   too low, and that either microbial emissions estimates are too high (Schwietzke et al., 2016), or that biomass burning

691   estimates are too high (Worden et al., 2017). We argue that greater analysis of δ^2H-CH$_4$ measurements could be valuable

692   for evaluating these and other emissions scenarios, as has been suggested previously (Rigby et al., 2012). This is

693   especially true for determining the relative proportion of fossil fuel and microbial emissions, since these sources have

694   widely differing δ^2H-CH$_4$ signatures (Table 1). Currently, atmospheric δ^2H-CH$_4$ measurements are not a routine

695   component of CH$_4$ monitoring programs, but we argue that based on both their value in constraining emissions sources

696   and sinks (Rigby et al., 2012), and the increasing practicality of high-frequency measurements (Chen et al.,

697   2016;Röckmann et al., 2016;Yacovitch et al., 2020), that there should be a renewed focus on these measurements.

698   The uncertainty in our bottom-up estimates, the overall greater uncertainty associated with isotopic source

699   signatures in our Monte Carlo calculations, and the apparent discrepancies for δ^{13}C-CH$_4$ shown in Figure 10, also imply

700   that isotopic source signatures for specific sources could be greatly improved. As noted by Rigby et al. (2012), the impact

701   of improved isotopic source signatures increases as measurement precision improves. We have discussed above the

702   importance of increased data assimilation and measurements from tropical wetlands, with a particular focus on C$_4$ plant

703   dominated ecosystems. Using the isotopic source signal uncertainties and emissions fluxes shown in Table 1, we

704   identified the sources with the greatest flux-weighted uncertainty in isotopic signatures. Based on this analysis, the

29

greatest uncertainty for global source δ^2H-CH$_4$ estimates comes from source signatures for enteric fermentation and manure, low-latitude wetlands, onshore geological emissions, low-latitude and mid-latitude inland waters, termites, and landfills. We identified the same source categories as having the greatest flux-weighted uncertainty for δ^{13}C-CH$_4$, with the exception of termites, but repeat the caveat that the underlying dataset is less comprehensive for δ^{13}C-CH$_4$. We argue that these source categories should be considered priorities for future emissions source isotopic characterization through data assimilation and additional measurements. As discussed in Sect. 3.5.1, evaluation of possible latitudinal variation in enteric fermentation and landfill δ^2H-CH$_4$ is particularly promising.

5 Conclusions

Our analysis of an expanded isotopic dataset for freshwater CH$_4$ confirms the previous finding that δ^2H-H$_2$O is the primary determinant of δ^2H-CH$_4$ on a global scale (Waldron et al., 1999a), but also finds that the slope of this relationship is probably flatter than was inferred previously (Fig. 3). This flatter slope is primarily the result of the inclusion of a much larger number of high-latitude sites with low δ^2H-H$_2$O our dataset. We find that the inferred relationship between δ^2H-CH$_4$ and δ^2H-H$_2$O is not highly sensitive to whether measured δ^2H-H$_2$O, modeled δ^2H$_p$, or a combination of the two (i.e. a best-estimate) is used to estimate δ^2H-H$_2$O. This implies that gridded datasets of δ^2H$_p$ or isotope-enabled climate models could be used to predict the distribution of δ^2H-CH$_4$ in the present, as well as under past and future climates. Our analysis also suggests that annual δ^2H$_p$ may be a better predictor for wetland δ^2H-CH$_4$, while seasonal δ^2H$_p$ may be a better predictor of inland water δ^2H-CH$_4$. The slope of δ^2H-CH$_4$ vs. δ^2H-H$_2$O in both wetlands and inland waters agrees well with that found in incubation experiments (Schoell, 1980;Sugimoto and Wada, 1995;Waldron et al., 1998;Waldron et al., 1999a), and we concur with previous inferences that this slope is partly controlled by variation in the δ^2H of acetate as a function of δ^2H-H$_2$O (Waldron et al., 1999a). Analysis of co-variation of δ^2H-CH$_{4,W0}$ with δ^{13}C-CH$_4$, δ^{13}C-CO$_2$, and α_C suggest that residual variation in δ^2H-CH$_4$ is influenced by a complex set of biogeochemical variables, including both variable isotopic fractionation related to methanogenesis, and post-production isotopic fractionation related to CH$_4$ oxidation and diffusive gas transport. A significant positive correlation between δ^2H-CH$_{4,W0}$ and both δ^{13}C-CO$_2$, and α_C in wetlands suggests that hydrogen isotope fractionation related to methanogenesis pathway or enzymatic reversibility may be more important in these environments, but this result is dependent on the method used to estimate δ^2H-H$_2$O and requires further validation.

The dependence of δ^2H-CH$_4$ on δ^2H-H$_2$O leads to clear latitudinal differences in δ^2H-CH$_4$, with particularly low values from high latitude sites (Fig. 4; Fig. 7A). The mechanism for latitudinal differences in δ^2H-CH$_4$ is distinct from proposed mechanisms for latitudinal differences in δ^{13}C-CH$_4$ (Ganesan et al., 2018), implying that these two isotopic tracers are complementary in differentiating geographic emissions sources. We estimate a global flux-weighted δ^2H-CH$_4$ signature from freshwater environments of -310±15‰, which is enriched relative to values used in previous source

30

apportionment studies (Rice et al., 2016;Bock et al., 2017). We observe a significantly higher δ^2H-CH$_{4,W0}$ distribution in inland waters relative to wetlands (Fig. 8A), which we suggest is a result of greater rates of CH$_4$ oxidation in inland waters. We do not find significant differences between more specific ecosystem categories, nor do we find significant differences in δ^2H-CH$_{4,W0}$ between sample types (Fig. 9A), with the exception of higher values in dissolved CH$_4$ relative to gas-phase CH$_4$ in inland water environments.

Our bottom-up estimate of the global δ^2H-CH$_4$ source signature, -278±15‰, is higher than previous bottom-up estimates (Whiticar and Schaefer, 2007), but is within the range of top-down estimates based on atmospheric measurements and modeled sink fractionations (Rice et al., 2016). In contrast, our bottom-up estimate of global δ^{13}C-CH$_4$, -56.4±2.6‰, is low relative to top-down estimates, which is partially explained by a lack of data from C$_4$ plant-dominated ecosystems in the freshwater CH$_4$ isotopic dataset. The agreement between bottom-up and top-down global δ^2H-CH$_4$ estimates suggests that our current understanding of δ^2H-CH$_4$ source signatures, when combined with inventory-based flux estimates (Saunois et al., 2020), is consistent with atmospheric measurements. This supports the argument that increased measurements and modeling of atmospheric δ^2H-CH$_4$ could help to constrain global CH$_4$ budgets (Rigby et al., 2012). However, there is clearly a need to better constrain source signatures for both δ^2H-CH$_4$ and δ^{13}C-CH$_4$, especially from low-latitude microbial sources.

769   **References**

770

771   Alstad, K. P., and Whiticar, M. J.: Carbon and hydrogen isotope ratio characterization of methane dynamics for Fluxnet
772   Peatland Ecosystems, Org Geochem, 42, 548-558, 2011.
773   Bastviken, D., Tranvik, L. J., Downing, J. A., Crill, P. M., and Enrich-Prast, A.: Freshwater methane emissions offset the
774   continental carbon sink, Science, 331, 50-50, 2011.
775   Bellisario, L., Bubier, J., Moore, T., and Chanton, J.: Controls on CH4 emissions from a northern peatland, Global
776   Biogeochem Cy, 13, 81-91, 1999.
777   Bergamaschi, P.: Seasonal variations of stable hydrogen and carbon isotope ratios in methane from a Chinese rice paddy,
778   Journal of Geophysical Research: Atmospheres, 102, 25383-25393, 1997.
779   Bilek, R., Tyler, S., Kurihara, M., and Yagi, K.: Investigation of cattle methane production and emission over a 24-hour
780   period using measurements of δ13C and δD of emitted CH4 and rumen water, Journal of Geophysical Research:
781   Atmospheres, 106, 15405-15413, 2001.
782   Bock, M., Schmitt, J., Möller, L., Spahni, R., Blunier, T., and Fischer, H.: Hydrogen isotopes preclude marine hydrate
783   CH4 emissions at the onset of Dansgaard-Oeschger events, Science, 328, 1686-1689, 2010.
784   Bock, M., Schmitt, J., Beck, J., Seth, B., Chappellaz, J., and Fischer, H.: Glacial/interglacial wetland, biomass burning,
785   and geologic methane emissions constrained by dual stable isotopic CH4 ice core records, Proceedings of the National
786   Academy of Sciences, 114, E5778-E5786, 2017.
787   Bouchard, F., Laurion, I., Preskienis, V., Fortier, D., Xu, X., and Whiticar, M.: Modern to millennium-old greenhouse
788   gases emitted from ponds and lakes of the Eastern Canadian Arctic (Bylot Island, Nunavut), Biogeosciences, 12, 7279-
789   7298, 2015.
790   Bowen, G. J., and Wilkinson, B.: Spatial distribution of δ18O in meteoric precipitation, Geology, 30, 315-318, 2002.
791   Bowen, G. J., and Revenaugh, J.: Interpolating the isotopic composition of modern meteoric precipitation, Water
792   Resources Research, 39, 2003.
793   Bowen, G. J., Wassenaar, L. I., and Hobson, K. A.: Global application of stable hydrogen and oxygen isotopes to wildlife
794   forensics, Oecologia, 143, 337-348, 2005.
795   Bowes, H. L., and Hornibrook, E. R.: Emission of highly 13C-depleted methane from an upland blanket mire, Geophys
796   Res Lett, 33, 2006.
797   Brooks, J. R., Gibson, J. J., Birks, S. J., Weber, M. H., Rodecap, K. D., and Stoddard, J. L.: Stable isotope estimates of
798   evaporation: inflow and water residence time for lakes across the United States as a tool for national lake water quality
799   assessments, Limnol Oceanogr, 59, 2150-2165, 2014.
800   Brosius, L., Walter Anthony, K., Grosse, G., Chanton, J., Farquharson, L., Overduin, P. P., and Meyer, H.: Using the
801   deuterium isotope composition of permafrost meltwater to constrain thermokarst lake contributions to atmospheric CH4
802   during the last deglaciation, Journal of Geophysical Research: Biogeosciences (2005–2012), 117, 2012.
803   Burke Jr, R.: SHALLOW AQUATIC SEDIMENTS, Bacterial Gas. Conference, Mila, September 25-26, 1989, 1992, 47,
804   Burke Jr, R. A., and Sackett, W. M.: Stable hydrogen and carbon isotopic compositions of biogenic methanes from
805   several shallow aquatic environments, in, ACS Publications, 1986.
806   Burke Jr, R. A., Barber, T. R., and Sackett, W. M.: Methane flux and stable hydrogen and carbon isotope composition of
807   sedimentary methane from the Florida Everglades, Global Biogeochem Cy, 2, 329-340, 1988.
808   Burke Jr, R. A., Barber, T. R., and Sackett, W. M.: Seasonal variations of stable hydrogen and carbon isotope ratios of
809   methane in subtropical freshwater sediments, Global Biogeochem Cy, 6, 125-138, 1992.
810   Burke Jr, R. A.: Possible influence of hydrogen concentration on microbial methane stable hydrogen isotopic
811   composition, Chemosphere, 26, 55-67, 1993.
812   Cadieux, S. B., White, J. R., Sauer, P. E., Peng, Y., Goldman, A. E., and Pratt, L. M.: Large fractionations of C and H
813   isotopes related to methane oxidation in Arctic lakes, Geochim Cosmochim Ac, 187, 141-155, 2016.
814   Chanton, J., Whiting, G., Blair, N., Lindau, C., and Bollich, P.: Methane emission from rice: Stable isotopes, diurnal
815   variations, and CO2 exchange, Global Biogeochem Cy, 11, 15-27, 1997.
816   Chanton, J. P.: The effect of gas transport on the isotope signature of methane in wetlands, Org Geochem, 36, 753-768,
817   2005.

32

818   Chanton, J. P., Fields, D., and Hines, M. E.: Controls on the hydrogen isotopic composition of biogenic methane from
819   high-latitude terrestrial wetlands, Journal of Geophysical Research: Biogeosciences (2005–2012), 111, 2006.
820   Chasar, L., Chanton, J., Glaser, P. H., and Siegel, D.: Methane concentration and stable isotope distribution as evidence
821   of rhizospheric processes: Comparison of a fen and bog in the Glacial Lake Agassiz Peatland complex, Annals of
822   Botany, 86, 655-663, 2000.
823   Chen, Y., Lehmann, K. K., Peng, Y., Pratt, L., White, J., Cadieux, S., Sherwood Lollar, B., Lacrampe-Couloume, G., and
824   Onstott, T. C.: Hydrogen Isotopic Composition of Arctic and Atmospheric CH4 Determined by a Portable Near-Infrared
825   Cavity Ring-Down Spectrometer with a Cryogenic Pre-Concentrator, Astrobiology, 16, 787-797, 2016.
826   Conrad, R., Noll, M., Claus, P., Klose, M., Bastos, W., and Enrich-Prast, A.: Stable carbon isotope discrimination and
827   microbiology of methane formation in tropical anoxic lake sediments, Biogeosciences, 8, 795, 2011.
828   Coplen, T. B.: Guidelines and recommended terms for expression of stable-isotope-ratio and gas-ratio measurement
829   results, Rapid Commun Mass Sp, 25, 2538-2560, 2011.
830   David, K., Timms, W., Hughes, C. E., Crawford, J., and McGeeney, D.: Application of the pore water stable isotope
831   method and hydrogeological approaches to characterise a wetland system, Hydrology and Earth System Sciences, 22,
832   6023-6041, 2018.
833   Douglas, P.M.J., Stolper, D., Smith, D., Walter Anthony, K., Paull, C., Dallimore, S., Wik, M., Crill, P., Winterdahl, M.,
834   Eiler, J., and Sessions, A. L.: Diverse origins of Arctic and Subarctic methane point source emissions identified with
835   multiply-substituted isotopologues, Geochim Cosmochim Ac, 188, 163-188, 2016.
836   Douglas, P.M.J., Stolper, D. A., Eiler, J. M., Sessions, A. L., Lawson, M., Shuai, Y., Bishop, A., Podlaha, O. G., Ferreira,
837   A. A., and Neto, E. V. S.: Methane clumped isotopes: progress and potential for a new isotopic tracer, Org Geochem,
838   113, 262-282, 2017.
839   Douglas, P.M.J., Gonzalez Moguel, R., Walter Anthony, K. M., Wik, M., Crill, P. M., Dawson, K. S., Smith, D. A.,
840   Yanay, E., Lloyd, M. K., and Stolper, D. A.: Clumped isotopes link older carbon substrates with slower rates of
841   methanogenesis in northern lakes, Geophys Res Lett, 47, e2019GL086756, 2020.
842   Douglas, P.M.J.; Stratigopoulos, E.; Park, J.; Phan, D.: Data for geographic variability in freshwater methane hydrogen
843   isotope ratios and its implications for emissions source apportionment and microbial biogeochemistry. figshare.
844   https://doi.org/10.6084/m9.figshare.13194833.v2
845   Drevon, D., Fursa, S. R., and Malcolm, A. L.: Intercoder reliability and validity of WebPlotDigitizer in extracting
846   graphed data, Behavior modification, 41, 323-339, 2017.
847   Dunn, O. J.: Multiple comparisons using rank sums, Technometrics, 6, 241-252, 1964.
848   Fisher, R. E., Sriskantharajah, S., Lowry, D., Lanoisellé, M., Fowler, C., James, R., Hermansen, O., Lund Myhre, C.,
849   Stohl, A., Greinert, J., and Nisbet, E. G.: Arctic methane sources: Isotopic evidence for atmospheric inputs, Geophys Res
850   Lett, 38, L21803, 2011.
851   Fletcher, D., and Dixon, P. M.: Modelling data from different sites, times or studies: weighted vs. unweighted regression,
852   Methods in Ecology and Evolution, 3, 168-176, 2012.
853   Ganesan, A., Stell, A., Gedney, N., Comyn-Platt, E., Hayman, G., Rigby, M., Poulter, B., and Hornibrook, E.: Spatially
854   resolved isotopic source signatures of wetland methane emissions, Geophys Res Lett, 45, 3737-3745, 2018.
855   Gruen, D. S., Wang, D. T., Könneke, M., Topçuoğlu, B. D., Stewart, L. C., Goldhammer, T., Holden, J. F., Hinrichs, K.-
856   U., and Ono, S.: Experimental investigation on the controls of clumped isotopologue and hydrogen isotope ratios in
857   microbial methane, Geochim Cosmochim Ac, 237, 339-356, 2018.
858   Happell, J. D., Chanton, J. P., Whiting, G. J., and Showers, W. J.: Stable isotopes as tracers of methane dynamics in
859   Everglades marshes with and without active populations of methane oxidizing bacteria, Journal of Geophysical Research:
860   Atmospheres, 98, 14771-14782, 1993.
861   Happell, J. D., Chanton, J. P., and Showers, W. S.: The influence of methane oxidation on the stable isotopic composition
862   of methane emitted from Florida swamp forests, Geochim Cosmochim Ac, 58, 4377-4388, 1994.
863   Hornibrook, E. R., Longstaffe, F. J., and Fyfe, W. S.: Spatial distribution of microbial methane production pathways in
864   temperate zone wetland soils: stable carbon and hydrogen isotope evidence, Geochim Cosmochim Ac, 61, 745-753,
865   1997.

866 Hornibrook, E. R.: The stable carbon isotope composition of methane produced and emitted from northern peatlands,
867 Baird, A., Belyea, L., Comas, X., Reeve, A., and Slater, L., American Geophysical Union, Geophysical Monograph
868 Series, 184, 187-203, 2009.
869 Huang, Y., Shuman, B., Wang, Y., and Webb III, T.: Hydrogen isotope ratios of palmitic acid in lacustrine sediments
870 record late Quaternary climate variations, Geology, 30, 1103-1106, 2002.
871 Jonsson, C. E., Leng, M. J., Rosqvist, G. C., Seibert, J., and Arrowsmith, C.: Stable oxygen and hydrogen isotopes in
872 sub-Arctic lake waters from northern Sweden, J Hydrol, 376, 143-151, 2009.
873 Kai, F. M., Tyler, S. C., Randerson, J. T., and Blake, D. R.: Reduced methane growth rate explained by decreased
874 Northern Hemisphere microbial sources, Nature, 476, 194-197, 2011.
875 Kruskal, W. H., and Wallis, W. A.: Use of ranks in one-criterion variance analysis, Journal of the American statistical
876 Association, 47, 583-621, 1952.
877 Krzycki, J., Kenealy, W., DeNiro, M., and Zeikus, J.: Stable carbon isotope fractionation by Methanosarcina barkeri
878 during methanogenesis from acetate, methanol, or carbon dioxide-hydrogen, Applied and Environmental Microbiology,
879 53, 2597-2599, 1987.
880 Lansdown, J., Quay, P., and King, S.: CH_4 production via CO_2 reduction in a temperate bog: A source of 13C-depleted
881 CH_4, Geochim Cosmochim Ac, 56, 3493-3503, 1992.
882 Lansdown, J. M.: The carbon and hydrogen stable isotope composition of methane released from natural wetlands and
883 ruminants, PhD Dissertation, University of Washington, 1992.
884 Lecher, A. L., Chuang, P. C., Singleton, M., and Paytan, A.: Sources of methane to an Arctic lake in Alaska: An isotopic
885 investigation, Journal of Geophysical Research: Biogeosciences, 122, 753-766, 2017.
886 Levin, I., Bergamaschi, P., Dörr, H., and Trapp, D.: Stable isotopic signature of methane from major sources in Germany,
887 Chemosphere, 26, 161-177, 1993.
888 Liptay, K., Chanton, J., Czepiel, P., and Mosher, B.: Use of stable isotopes to determine methane oxidation in landfill
889 cover soils, Journal of Geophysical Research: Atmospheres, 103, 8243-8250, 1998.
890 Mann, H. B., and Whitney, D. R.: On a test of whether one of two random variables is stochastically larger than the
891 other, The annals of mathematical statistics, 50-60, 1947.
892 Marik, T., Fischer, H., Conen, F., and Smith, K.: Seasonal variations in stable carbon and hydrogen isotope ratios in
893 methane from rice fields, Global Biogeochem Cy, 16, 41-41-41-11, 2002.
894 Martens, C. S., Kelley, C. A., Chanton, J. P., and Showers, W. J.: Carbon and hydrogen isotopic characterization of
895 methane from wetlands and lakes of the Yukon-Kuskokwim delta, western Alaska, Journal of Geophysical Research:
896 Atmospheres (1984–2012), 97, 16689-16701, 1992.
897 Miles, N. L., Martins, D. K., Richardson, S. J., Rella, C. W., Arata, C., Lauvaux, T., Davis, K. J., Barkley, Z. R.,
898 McKain, K., and Sweeney, C.: Calibration and field testing of cavity ring-down laser spectrometers measuring CH 4, CO
899 2, and δ 13 CH 4 deployed on towers in the Marcellus Shale region, Atmospheric Measurement Techniques, 11, 1273-
900 1295, 2018.
901 Mischler, J. A., Sowers, T. A., Alley, R. B., Battle, M., McConnell, J., Mitchell, L., Popp, T., Sofen, E., and Spencer, M.:
902 Carbon and hydrogen isotopic composition of methane over the last 1000 years, Global Biogeochem Cy, 23, 2009.
903 Mora, G., and Zanazzi, A.: Hydrogen isotope ratios of moss cellulose and source water in wetlands of Lake Superior,
904 United States reveal their potential for quantitative paleoclimatic reconstructions, Chem Geol, 468, 75-83, 2017.
905 Nakagawa, F., Yoshida, N., Sugimoto, A., Wada, E., Yoshioka, T., Ueda, S., and Vijarnsorn, P.: Stable isotope and
906 radiocarbon compositions of methane emitted from tropical rice paddies and swamps in Southern Thailand,
907 Biogeochemistry, 61, 1-19, 2002a.
908 Nakagawa, F., Yoshida, N., Nojiri, Y., and Makarov, V.: Production of methane from alasses in eastern Siberia:
909 Implications from its 14C and stable isotopic compositions, Global Biogeochem Cy, 16, 14-11-14-15, 2002b.
910 Nisbet, E., Dlugokencky, E., Manning, M., Lowry, D., Fisher, R., France, J., Michel, S., Miller, J., White, J., and
911 Vaughn, B.: Rising atmospheric methane: 2007–2014 growth and isotopic shift, Global Biogeochem Cy, 30, 1356-1370,
912 2016.
913 Nisbet, E. G., Manning, M., Dlugokencky, E., Fisher, R., Lowry, D., Michel, S., Myhre, C. L., Platt, S. M., Allen, G.,
914 and Bousquet, P.: Very strong atmospheric methane growth in the 4 years 2014–2017: Implications for the Paris
915 Agreement, Global Biogeochem Cy, 33, 318-342, 2019.

916   Penger, J., Conrad, R., and Blaser, M.: Stable carbon isotope fractionation by methylotrophic methanogenic archaea,
917   Applied and environmental microbiology, 78, 7596-7602, 2012.
918   Penning, H., Plugge, C. M., Galand, P. E., and Conrad, R.: Variation of carbon isotope fractionation in hydrogenotrophic
919   methanogenic microbial cultures and environmental samples at different energy status, Global Change Biol, 11, 2103-
920   2113, 2005.
921   Penning, H., and Conrad, R.: Quantification of carbon flow from stable isotope fractionation in rice field soils with
922   different organic matter content, Org Geochem, 38, 2058-2069, 2007.
923   Pine, M. J., and Barker, H.: Studies on the methane fermentation XII.: The pathway of hydrogen in the acetate
924   fermentation, Journal of Bacteriology, 71, 644-648, 1956.
925   Pison, I., Ringeval, B., Bousquet, P., Prigent, C., and Papa, F.: Stable atmospheric methane in the 2000s: key-role of
926   emissions from natural wetlands, 2013.
927   Popp, T. J., Chanton, J. P., Whiting, G. J., and Grant, N.: Methane stable isotope distribution at a Carex dominated fen in
928   north central Alberta, Global Biogeochem Cy, 13, 1063-1077, 1999.
929   Rice, A. L., Butenhoff, C. L., Teama, D. G., Röger, F. H., Khalil, M. A. K., and Rasmussen, R. A.: Atmospheric methane
930   isotopic record favors fossil sources flat in 1980s and 1990s with recent increase, Proceedings of the National Academy
931   of Sciences, 113, 10791-10796, 2016.
932   Rigby, M., Manning, A., and Prinn, R.: The value of high-frequency, high-precision methane isotopologue
933   measurements for source and sink estimation, Journal of Geophysical Research: Atmospheres, 117, 2012.
934   Röckmann, T., Eyer, S., Van Der Veen, C., Popa, M. E., Tuzson, B., Monteil, G., Houweling, S., Harris, E., Brunner, D.,
935   and Fischer, H.: In situ observations of the isotopic composition of methane at the Cabauw tall tower site, Atmos. Chem.
936   Phys., 16, 10469-10487, 2016.
937   Rozanski, K., Araguás-Araguás, L., and Gonfiantini, R.: Isotopic patterns in modern global precipitation, Geophysical
938   Monograph Series, 78, 1-36, 1993.
939   Sachse, D., Billault, I., Bowen, G. J., Chikaraishi, Y., Dawson, T. E., Feakins, S. J., Freeman, K. H., Magill, C. R.,
940   McInerney, F. A., and van der Meer, M. T. J.: Molecular paleohydrology: Interpreting the hydrogen-isotopic composition
941   of lipid biomarkers from photosynthesizing organisms, Annual Review of Earth and Planetary Sciences, 40, 221-249,
942   2012.
943   Sakagami, H., Takahashi, N., Hachikubo, A., Minami, H., Yamashita, S., Shoji, H., Khlystov, O., Kalmychkov, G.,
944   Grachev, M., and De Batist, M.: Molecular and isotopic composition of hydrate-bound and dissolved gases in the
945   southern basin of Lake Baikal, based on an improved headspace gas method, Geo-Mar Lett, 32, 465-472, 2012.
946   Saunois, M., Stavert, A. R., Poulter, B., Bousquet, P., Canadell, J. G., Jackson, R. B., Raymond, P. A., Dlugokencky, E.
947   J., Houweling, S., and Patra, P. K.: The global methane budget 2000–2017, Earth System Science Data, 12, 1561-1623,
948   2020.
949   Schaefer, H., Fletcher, S. E. M., Veidt, C., Lassey, K. R., Brailsford, G. W., Bromley, T. M., Dlugokencky, E. J., Michel,
950   S. E., Miller, J. B., and Levin, I.: A 21st-century shift from fossil-fuel to biogenic methane emissions indicated by
951   13CH4, Science, 352, 80-84, 2016.
952   Schoell, M.: The hydrogen and carbon isotopic composition of methane from natural gases of various origins, Geochim
953   Cosmochim Ac, 44, 649-661, 1980.
954   Schoell, M.: Genetic characterization of natural gases, AAPG bulletin, 67, 2225-2238, 1983.
955   Schwietzke, S., Sherwood, O. A., Bruhwiler, L. M., Miller, J. B., Etiope, G., Dlugokencky, E. J., Michel, S. E., Arling,
956   V. A., Vaughn, B. H., and White, J. W.: Upward revision of global fossil fuel methane emissions based on isotope
957   database, Nature, 538, 88-91, 2016.
958   Shapiro, S. S., and Wilk, M. B.: An analysis of variance test for normality (complete samples), Biometrika, 52, 591-611,
959   1965.
960   Sherwood, O. A., Schwietzke, S., Arling, V. A., and Etiope, G.: Global inventory of gas geochemistry data from fossil
961   fuel, microbial and burning sources, version 2017, Earth System Science Data, 9, 2017.
962   Shoemaker, J., Varner, R., and Schrag, D.: Characterization of subsurface methane production and release over 3 years at
963   a New Hampshire wetland, Geochim Cosmochim Ac, 91, 120-139, 2012.
964   Sprenger, M., Tetzlaff, D., Tunaley, C., Dick, J., and Soulsby, C.: Evaporation fractionation in a peatland drainage
965   network affects stream water isotope composition, Water Resources Research, 53, 851-866, 2017.

35

966 Stell, A. C., Douglas, P.M.J., Rigby, M., and Ganesan, A.L.: The impact of spatially varying wetland source signatures
967 on the atmospheric variability of δD-CH$_4$, Philosophical Transactions of the Royal Society A. Accepted article in press,
968 2021.
969 Stolper, D., Martini, A., Clog, M., Douglas, P., Shusta, S., Valentine, D., Sessions, A., and Eiler, J.: Distinguishing and
970 understanding thermogenic and biogenic sources of methane using multiply substituted isotopologues, Geochim
971 Cosmochim Ac, 161, 219-247, 2015.
972 Sugimoto, A., and Wada, E.: Hydrogen isotopic composition of bacterial methane: CO$_2$/H$_2$ reduction and acetate
973 fermentation, Geochim Cosmochim Ac, 59, 1329-1337, 1995.
974 Teasdale, C. J., Hall, J. A., Martin, J. P., and Manning, D. A.: Discriminating methane sources in ground gas emissions in
975 NW England, Quarterly Journal of Engineering Geology and Hydrogeology, 52, 110-122, 2019.
976 Thompson, H. A., White, J. R., Pratt, L. M., and Sauer, P. E.: Spatial variation in flux, δ 13 C and δ 2 H of methane in a
977 small Arctic lake with fringing wetland in western Greenland, Biogeochemistry, 131, 17-33, 2016.
978 Thompson, K. M., Burmaster, D. E., and Crouch3, E. A.: Monte Carlo techniques for quantitative uncertainty analysis in
979 public health risk assessments, Risk Analysis, 12, 53-63, 1992.
980 Thompson, R. L., Nisbet, E., Pisso, I., Stohl, A., Blake, D., Dlugokencky, E., Helmig, D., and White, J.: Variability in
981 atmospheric methane from fossil fuel and microbial sources over the last three decades, Geophys Res Lett, 45, 11,499-
982 411,508, 2018.
983 Turner, A. J., Frankenberg, C., and Kort, E. A.: Interpreting contemporary trends in atmospheric methane, Proceedings of
984 the National Academy of Sciences, 116, 2805-2813, 2019.
985 Tyler, J. J., Leng, M. J., and Arrowsmith, C.: Seasonality and the isotope hydrology of Lochnagar, a Scottish mountain
986 lake: implications for palaeoclimate research, The Holocene, 17, 717-727, 2007.
987 Tyler, S., Bilek, R., Sass, R., and Fisher, F.: Methane oxidation and pathways of production in a Texas paddy field
988 deduced from measurements of flux, δl3C, and δD of CH4, Global Biogeochem Cy, 11, 323-348, 1997.
989 Umezawa, T., Aoki, S., Kim, Y., Morimoto, S., and Nakazawa, T.: Carbon and hydrogen stable isotopic ratios of
990 methane emitted from wetlands and wildfires in Alaska: Aircraft observations and bonfire experiments, Journal of
991 Geophysical Research: Atmospheres, 116, 2011.
992 Valentine, D., Sessions, A., Tyler, S., and Chidthaisong, A.: Hydrogen isotope fractionation during H2/CO2
993 acetogenesis: hydrogen utilization efficiency and the origin of lipid-bound hydrogen, Geobiology, 2, 179-188, 2004a.
994 Valentine, D. L., Chidthaisong, A., Rice, A., Reeburgh, W. S., and Tyler, S. C.: Carbon and hydrogen isotope
995 fractionation by moderately thermophilic methanogens, Geochim Cosmochim Ac, 68, 1571-1590, 2004b.
996 Vigano, I., Holzinger, R., Keppler, F., Greule, M., Brand, W. A., Geilmann, H., Van Weelden, H., and Röckmann, T.:
997 Water drives the deuterium content of the methane emitted from plants, Geochim Cosmochim Ac, 74, 3865-3873, 2010.
998 Wahlen, M.: Carbon dioxide, carbon monoxide and methane in the atmosphere: abundance and isotopic composition,
999 Stable isotopes in ecology and environmental science, 93-113, 1994.
1000 Waldron, S., Watson-Craik, I. A., Hall, A. J., and Fallick, A. E.: The carbon and hydrogen stable isotope composition of
1001 bacteriogenic methane: a laboratory study using a landfill inoculum, Geomicrobiology Journal, 15, 157-169, 1998.
1002 Waldron, S., Lansdown, J., Scott, E., Fallick, A., and Hall, A.: The global influence of the hydrogen iostope composition
1003 of water on that of bacteriogenic methane from shallow freshwater environments, Geochim Cosmochim Ac, 63, 2237-
1004 2245, 1999a.
1005 Waldron, S., Hall, A. J., and Fallick, A. E.: Enigmatic stable isotope dynamics of deep peat methane, Global Biogeochem
1006 Cy, 13, 93-100, 1999b.
1007 Walter, K., Chanton, J. P., Chapin, F. S., Schuur, E. A. G., and Zimov, S. A.: Methane production and bubble emissions
1008 from arctic lakes: Isotopic implications for source pathways and ages, J Geophys Res-Biogeo, 113, 2008.
1009 Walter, K. M., Zimov, S., Chanton, J. P., Verbyla, D., and Chapin, F. S.: Methane bubbling from Siberian thaw lakes as a
1010 positive feedback to climate warming, Nature, 443, 71-75, 2006.
1011 Wang, D. T., Gruen, D. S., Sherwood Lollar, B., Hinrichs, K.-U., Stewart, L. C., Holden, J. F., Hristov, A. N., Pohlman,
1012 J. W., Morrill, P. L., Könneke, M., Delwiche, K. B., Reeves, E. P., Sutcliffe, C. N., Ritter, D. J., Seewald, J. S.,
1013 McIntosh, J. C., Hemond, H. F., Kubo, M. D., Cardace, D., Hoehler, T. M., and Ono, S.: Nonequilibrium clumped
1014 isotope signals in microbial methane, Science, 348, 428-431, 2015.

1015   Wang, D. T., Welander, P. V., and Ono, S.: Fractionation of the methane isotopologues $^{13}CH_4$, $^{12}CH_3D$, and $^{13}CH_3D$
1016   during aerobic oxidation of methane by *Methylococcus capsulatus* (Bath), Geochim Cosmochim Ac, 192, 186-202, 2016.
1017   Wassmann, R., Thein, U., Whiticar, M., Rennenburg, H., Seiler, W., and Junk, W.: Methane emissions from the Amazon
1018   floodplain: characterization of production and transport, Global Biogeochem Cy, 6, 3-13, 1992.
1019   Whiticar, M., and Schaefer, H.: Constraining past global tropospheric methane budgets with carbon and hydrogen isotope
1020   ratios in ice, Philosophical Transactions of the Royal Society A: Mathematical, Physical and Engineering Sciences, 365,
1021   1793-1828, 2007.
1022   Whiticar, M. J., Faber, E., and Schoell, M.: Biogenic methane formation in marine and freshwater environments: CO_2
1023   reduction *vs.* acetate fermentation—Isotope evidence, Geochim Cosmochim Ac, 50, 693-709, 1986.
1024   Whiticar, M. J.: Carbon and hydrogen isotope systematics of bacterial formation and oxidation of methane, Chem Geol,
1025   161, 291-314, 1999.
1026   Woltemate, I., Whiticar, M., and Schoell, M.: Carbon and hydrogen isotopic composition of bacterial methane in a
1027   shallow freshwater lake, Limnol Oceanogr, 29, 985-992, 1984.
1028   Worden, J. R., Bloom, A. A., Pandey, S., Jiang, Z., Worden, H. M., Walker, T. W., Houweling, S., and Röckmann, T.:
1029   Reduced biomass burning emissions reconcile conflicting estimates of the post-2006 atmospheric methane budget,
1030   Nature communications, 8, 1-11, 2017.
1031   Yacovitch, T. I., Daube, C., and Herndon, S. C.: Methane emissions from offshore oil and gas platforms in the Gulf of
1032   Mexico, Environmental Science & Technology, 54, 3530-3538, 2020.
1033   Young, E., Kohl, I., Sherwood Lollar, B., Etiope, G., Rumble, D., Li, S., Haghnegahdar, M., Schauble, E., McCain, K.,
1034   Foustoukos, D., Sutclife, C., Warr, O., and Ballentine, C.: The relative abundances of resolved CH_2D_2 and $^{13}CH_3D$ and
1035   mechanisms controlling isotopic bond ordering in abiotic and biotic methane gases, Geochim Cosmochim Ac, 203, 2017.
1036   Yvon-Durocher, G., Allen, A. P., Bastviken, D., Conrad, R., Gudasz, C., St-Pierre, A., Thanh-Duc, N., and Del Giorgio,
1037   P. A.: Methane fluxes show consistent temperature dependence across microbial to ecosystem scales, Nature, 507, 488-
1038   491, 2014.
1039   Zazzeri, G., Lowry, D., Fisher, R., France, J., Lanoisellé, M., and Nisbet, E.: Plume mapping and isotopic
1040   characterisation of anthropogenic methane sources, Atmos Environ, 110, 151-162, 2015.
1041   Zhu, J., Liu, Z., Brady, E., Otto-Bliesner, B., Zhang, J., Noone, D., Tomas, R., Nusbaumer, J., Wong, T., and Jahn, A.:
1042   Reduced ENSO variability at the LGM revealed by an isotope-enabled Earth system model, Geophys Res Lett, 44, 6984-
1043   6992, 2017.
1044   Zimov, S., Voropaev, Y. V., Semiletov, I., Davidov, S., Prosiannikov, S., Chapin, F. S., Chapin, M., Trumbore, S., and
1045   Tyler, S.: North Siberian lakes: a methane source fueled by Pleistocene carbon, Science, 277, 800-802, 1997.
1046